Clim. Past, 18, 525–546, 2022
https://doi.org/10.5194/cp-18-525-2022

Climate of the Past
Open Access
EGU

Eocene to Oligocene vegetation and climate in the Tasmanian Gateway region were controlled by changes in ocean currents and pCO_2

Michael Amoo[1], Ulrich Salzmann[1], Matthew J. Pound[1], Nick Thompson[1], and Peter K. Bijl[2]

[1]Department of Geography and Environmental Sciences, Northumbria University, Newcastle upon Tyne, UK
[2]Marine Palynology and Palaeoceanography, Utrecht University, Princetonlaan 8A, Utrecht, the Netherlands

Correspondence: Michael Amoo (michael.amoo@northumbria.ac.uk)

Received: 1 October 2021 – Discussion started: 18 October 2021
Revised: 13 February 2022 – Accepted: 18 February 2022 – Published: 22 March 2022

Abstract. Considered one of the most significant climate reorganizations of the Cenozoic period, the Eocene–Oligocene Transition (EOT; ca. 34.44–33.65) is characterized by global cooling and the first major glacial advance on Antarctica. In the southern high latitudes, the EOT cooling is primarily recorded in the marine realm, and its extent and effect on the terrestrial climate and vegetation are poorly documented. Here, we present new, well-dated, continuous, high-resolution palynological (sporomorph) data and quantitative sporomorph-based climate estimates recovered from the East Tasman Plateau (ODP Site 1172) to reconstruct climate and vegetation dynamics from the late Eocene (37.97 Ma) to the early Oligocene (33.06 Ma). Our results indicate three major climate transitions and four vegetation communities occupying Tasmania under different precipitation and temperature regimes: (i) a warm-temperate *Nothofagus*–Podocarpaceae-dominated rainforest with paratropical elements from 37.97 to 37.52 Ma; (ii) a cool-temperate *Nothofagus*-dominated rainforest with secondary Podocarpaceae rapidly expanding and taking over regions previously occupied by the warmer taxa between 37.306 and 35.60 Ma; (iii) fluctuation between warm-temperate–paratropical taxa and cool temperate forest from 35.50 to 34.49 Ma, followed by a cool phase across the EOT (34.30–33.82 Ma); and (iv) a post-EOT (earliest Oligocene) recovery characterized by a warm-temperate forest association from 33.55 to 33.06 Ma. Coincident with changes in the stratification of water masses and sequestration of carbon from surface water in the Southern Ocean, our sporomorph-based temperature estimates between 37.52 and 35.60 Ma (phase ii) showed 2–3 °C terrestrial cooling. The unusual fluctuation between warm and cold temperate forest between 35.50 to 34.59 Ma is suggested to be linked to the initial deepening of the Tasmanian Gateway, allowing eastern Tasmania to come under the influence of warm water associated with the proto-Leeuwin Current (PLC). Further to the above, our terrestrial data show the mean annual temperature declining by about 2 °C across the EOT before recovering in the earliest Oligocene. This phenomenon is synchronous with regional and global cooling during the EOT and linked to declining pCO_2. However, the earliest Oligocene climate rebound along eastern Tasmania is linked to a transient recovery of atmospheric pCO_2 and sustained deepening of the Tasmanian Gateway, promoting PLC throughflow. The three main climate transitional events across the studied interval (late Eocene–earliest Oligocene) in the Tasmanian Gateway region suggest that changes in ocean circulation due to accelerated deepening of the Tasmanian Gateway may not have been solely responsible for the changes in terrestrial climate and vegetation dynamics; a series of regional and global events, including a change in the stratification of water masses, sequestration of carbon from surface waters, and changes in pCO_2, may have also played vital roles.

1 Introduction

Palynological reconstruction demonstrates a high sensitivity of global vegetation to past changes in climate, leading to major shifts in biome distribution (Pound and Salzmann, 2017). The Eocene–Oligocene Transition (EOT; 34.44–33.65 Ma; Katz et al., 2008; Hutchinson et al., 2021) is one of

the most important climate transitions of the Cenozoic and is characterized by a shift from largely ice-free greenhouse conditions to an icehouse climate, involving the development of the Antarctic cryosphere and global cooling (Liu et al., 2009; Pearson et al., 2009; Pagani et al., 2011; Hutchinson et al., 2021).

Tectonic opening of the southern gateways (Kennett, 1977) and a large and sharp drop in global atmospheric CO_2 (DeConto and Pollard, 2003; Huber et al., 2004; Zachos et al., 2008; Goldner et al., 2014; Ladant et al., 2014) have been proposed as possible drivers for this climate transition. The opening of the Australian–Antarctic Seaway (Tasmanian Gateway) and the Drake Passage led to the strengthening of the Antarctic Circumpolar Current (ACC), which thermally isolated Antarctica (Kennett, 1977). However, marine geology, micropalaeontology, and model simulation showed a potential time lag between the onset of the ACC and palaeogeographic changes, hence challenging global climate change at the EOT driven by Southern Hemisphere tectonics (Huber et al., 2004; Stickley et al., 2004; Goldner et al., 2014).

Although southern gateway opening and deepening have failed to fully explain Antarctic cooling at the EOT, the oceanographic changes following gateway opening and deepening have been reported to climatically impact Southern Ocean surface waters regionally (Stickley et al., 2004; Sijp et al., 2011; Houben et al., 2019; López-Quirós et al., 2021; Thompson et al., 2022). However, the extent and effect of the opening and deepening of the Tasmanian Gateway and its associated oceanographic changes on the coeval terrestrial climate and vegetation are not readily known. The lack of continuous and well-dated EOT terrestrial records place considerable limitations on the detailed temporal and spatial reconstruction of vegetation and climate. These challenges are further compounded by the fact that the few late Eocene and early Oligocene terrestrial palynoflora records indicate a rather heterogeneous vegetation response at the EOT (Pound and Salzmann, 2017). For example, in southeastern Australia, the late Eocene to early Oligocene vegetation records indicate a shift from a warm-temperate to a cool-temperate rainforest (Korasidis et al., 2019; Lauretano et al., 2021), whereas in New Zealand, a warm humid rainforest persisted (Pocknall, 1989; Homes et al., 2015; Prebble et al., 2021). East Antarctica (Prydz Bay) saw the collapse of tall woody vegetation and their replacement by impoverished, taiga-like vegetation with dwarfed trees before the EOT during the late Eocene (Macphail and Truswell, 2004; Truswell and Macphail, 2009; Tibbett et al., 2021), whereas a major vegetation change did not take place across the Drake Passage region until the early Oligocene, where there is a distinct expansion of gymnosperms and cryptogams, indicating glacial expansion (Thompson et al., 2022).

To further our understanding of the timing and potential drivers of southern high-latitude terrestrial environment change at the EOT, this study presents a new sporomorph record recovered from ODP Site 1172 (Fig. 1) on the East Tasman Plateau (ETP) spanning the late Eocene (37.97 Ma) to earliest Oligocene (33.06 Ma). The proximity of our study site to the Tasmanian Gateway places it in an excellent geographical position to identify potential climate or tectonic impacts on terrestrial vegetation of the Australo-Antarctica region. To further investigate potential links between the terrestrial and marine realm, we also compare our pollen-based quantitative climate estimates with newly published TEX_{86}-based sea-surface temperature (SST) and mean annual air temperature ($MAAT_{soil}$) reconstructions from the same site (Bijl et al., 2021). Our study reveals a significant terrestrial cooling $\sim$ 3 Myr prior to the EOT, and a warming in the earliest Oligocene that is most likely controlled by transient rebound of atmospheric pCO_2 and sustained deepening of the Tasmanian Gateway.

2 Materials and methods

2.1 Tectonic evolution and depositional setting

Continental breakup and seafloor spreading between Australia and the continental blocks of Lord Howe Rise, Campbell Plateau, and New Zealand (LCNZ) started in the Late Cretaceous ($\sim$ 75 Ma; Cande and Stock, 2004). Northward movement of Australia was propagated by rifting leading to the formation of the Tasman Sea and the separation of northeastern Australia in the Paleocene ($\sim$ 60 Ma; Gaina et al., 1999). The series of tectonic events paved the way for major ocean currents to flow along the coasts of eastern Australia and Tasmania, the ETP, and the South Tasman Rise (STR; Exon et al., 2004a). However, the Tasman promontory remained and separated the Australo-Antarctic Gulf (AAG) from the Pacific Ocean until the late Eocene ($\sim$ 35.5 Ma; Stickley et al., 2004). Our study site (ODP Site 1172 on the ETP; Fig. 1) is located on one of the four continental blocks sampled during ODP Leg 189 (Exon et al., 2004b) $\sim$ 170 km southeast of Tasmania (43°57.6′ S, 149°55.7′ E; Fig. 1a; Shipboard Scientific Party, 2001) at water depths of $\sim$ 2620 m (Exon et al., 2004a) and is enclosed by an 1800 m high seamount (Royer and Rollet, 1997). Prior to the Tasman Sea break-up in the Late Cretaceous (95 Ma), the ETP (which presently forms an oval platform) was part of Tasmania and the STR (Royer and Rollet, 1997; Exon et al., 2004b) and subsided slowly until the late Eocene. Bathymetric studies indicate that the ETP is connected to the east coast of Tasmania by the East Tasman Saddle (Royer and Rollet, 1997), which gives no indication of a deep basin in between (Hill and Exon, 2004). A dredging exercise confirmed the continental origin of the plateau (Exon et al., 1997). However, the age of the guyot/seamount (dated as 36 Ma; Lanyon et al., 1993) disqualifies the ETP itself from being the potential source of the terrestrial organic matter (Bijl et al., 2021). In addition, common Permo-Triassic reworked elements in our late Eocene–early Oligocene sporomorph assemblage likely indicate an eastern Tasmanian sporomorph

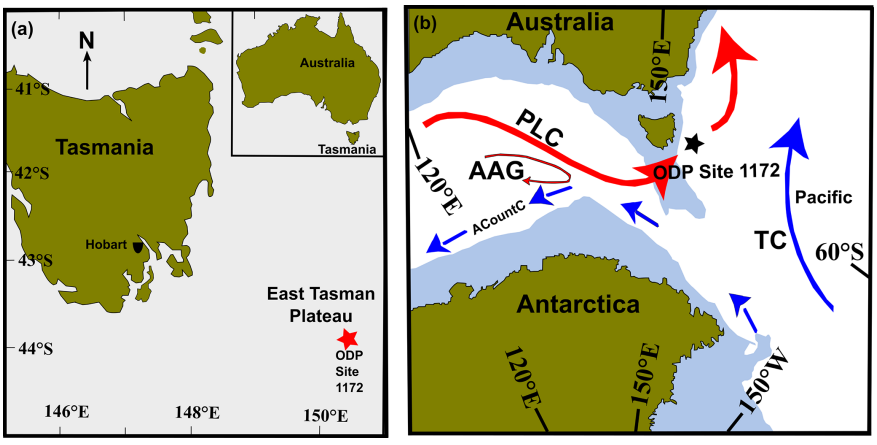

Figure 1. **(a)** Location of the East Tasman Plateau (ODP Site 1172; red star) and present-day Tasmania (Quilty, 2001). The Tasmania landmass is shown in green and the submerged ODP Site 1172 in grey, at a water depth of ∼ 2620 m. **(b)** Early Oligocene palaeogeography and palaeoceanography of the Tasmanian Gateway. ODP Site 1172 is marked by a five-pointed black star. Surface currents are modified after reconstructions by Stickley et al. (2004). TC: Tasman current, PLC: proto-Leeuwin current, ACountC: Antarctic Counter Current, AAG: Australo-Antarctic Gulf. Solid red arrows indicate warmer ocean currents from the AAG, and solid blue arrows indicate cooler ocean currents. Arrow size indicates the relative strength of the current. Figure is modified after Hoem et al. (2021).

source, in line with the Permian–Triassic upper Parmeener Group that contains terrestrial deposits and presently makes up the surface lithology across east Tasmania. A previous Paleocene–Eocene sporomorph assemblage from the ETP (ODP Site 1172) further supports an eastern Tasmanian terrestrial palynomorph source (Contreras et al., 2014).

Lithologically, the marine sedimentary record is divided into three units: (i) shallow-marine, organic-rich middle Eocene to lower upper Eocene clay; (ii) a highly condensed middle upper Eocene to lowermost Oligocene glauconite-rich, shallow-marine silty sandstone; and (iii) lower Oligocene siliceous-rich carbonate ooze (Stickley et al., 2004; Exon et al., 2001). Holes A and D of ODP Site 1172 on the East Tasman Plateau both yielded EOT records and have been analysed for their pollen and spore contents. The age model relies on magnetostratigraphy (which has a particularly clear signal in the late Eocene; Stickley et al., 2004; Fuller and Touchard, 2004) and biostratigraphy (dinoflagellate cysts, nannoplankton, and diatoms; Stickley et al., 2004; Bijl et al., 2013), as presented in Houben et al. (2019) and Bijl et al. (2021).

2.2 Study material

A total of 66 samples from the late Eocene to the earliest Oligocene of ODP Site 1172 (37.97–33.06 Ma) were analysed for terrestrial palynomorphs to reconstruct the palaeovegetation and palaeoclimate. Raw pollen data, including data on non-pollen palynomorphs (NPPs) and reworked sporomorphs, are available from the Zenodo data repository (Amoo et al., 2021). These samples were prepared at the Laboratory of Palaeobotany and Palynology, Utrecht University, following standard palynological processing techniques (Bijl et al., 2013). Sample processing involved treatment with 30 % HCl and 38 % HF and sieving the residues through a 15 µm nylon mesh (Pross, 2001). The residues were mounted onto microscope slides with glycerine gel used as the mounting medium. When analysing marine sediments such as those used in this study, sieving is a standard technique that is required to remove unwanted organic/inorganic matter and to increase the pollen concentration. To reduce the potential risk of losing small pollen grains, we regularly monitored our residues sieved at 10 and 15 µm mesh size. We found no evidence of a selective loss of smaller pollen grains such as *Myrtaceidites* and *Sapotaceoidaepollenites* cf. *latizonatus*. Similar to pollen records recovered from lakes (diameter > 200 m) and estuaries in Australia, our marine sporomorph record is likely to be biased towards abundant taxa in the regional vegetation, whereas sporomorphs recovered from coal, lignite, peat, and backswamp deposits are more likely to reflect local flora, with higher diversity and occasional high values of underrepresented taxa (Macphail et al., 1994).

Leica DM 500 and DM 2000 LED microscopes were used to analyse two slides for each sample at ×400 or ×1000 magnification. Where possible, 300 fossil spores and pollen grains (excluding reworked sporomorphs) were analysed for each sample, followed by further scanning of the entire microscope slide to record rare taxa. Aside from nine samples with counts below 50 grains, overall pollen preservation and counts were generally good. Reworked sporomorphs were identified based on the thermal maturation (colour) of their outer coat (exine) and occurrence outside their known stratigraphic range. Non-pollen palynomorphs were recorded but not added to the total pollen counts. Sporomorph percentages were calculated based on the total sum of pollen and

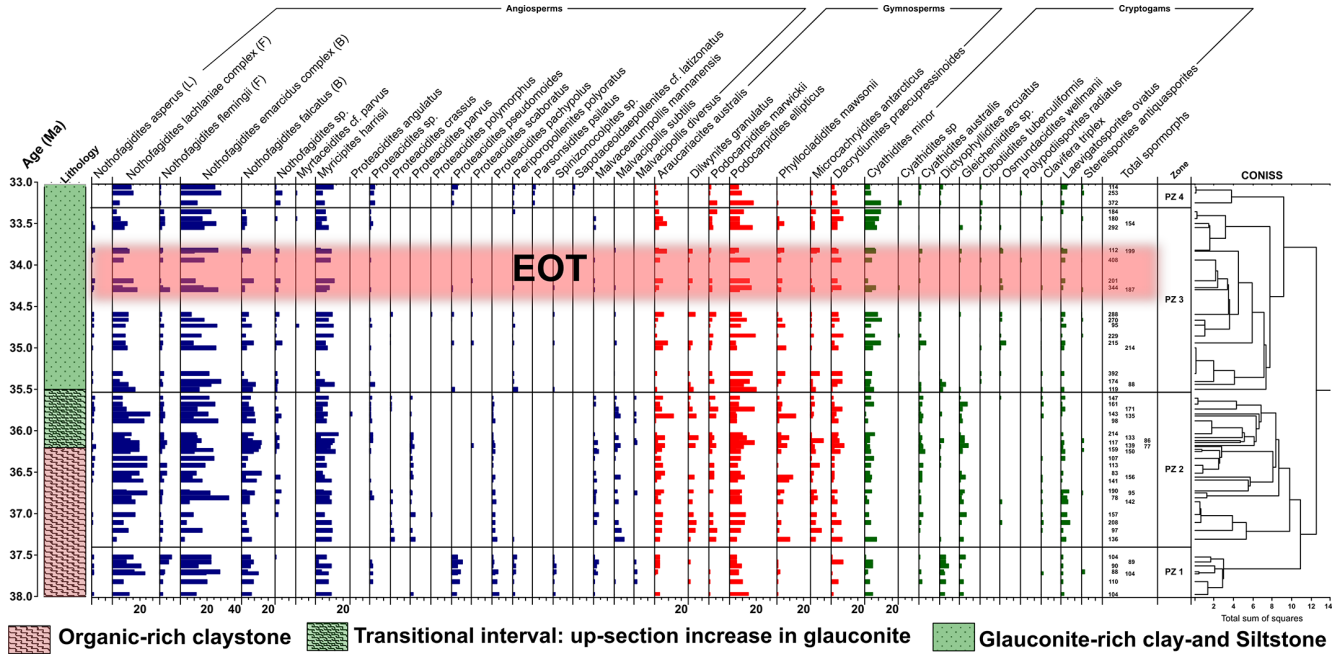

Figure 2. Sporomorph assemblages and relative abundances of major sporomorph taxa (angiosperms, gymnosperms, cryptogams) recovered from the late Eocene–early Oligocene of ODP Site 1172. Angiosperm relative abundances are marked by blue bars, gymnosperm relative abundances by red bars, and cryptogam relative abundances by green bars. In the angiosperm group, *Nothofagidites* is further divided into subgenera. These are *Brassospora* (B), *Fuscospora* (F), and *Lophozonia* (L) types. CONISS ordination constrains our late Eocene–early Oligocene sporomorph assemblages into four distinct pollen zones (PZ 1–PZ 4) or vegetation and climate phases. The age model is after Houben et al. (2019) and Bijl et al. (2021).

spores excluding reworked grains, and were plotted using Tilia version 2.6.1 (Fig. 2; Grimm, 1990). Using the Edwards and Cavalli-Sforza chord distance, we applied a stratigraphically constrained incremental sum-of-squares cluster analysis (CONISS; Grimm, 1987) to determine pollen assemblage zones (PZ; Fig. 2). Sporomorph identification and botanical affinities (used for nearest living relative identification of fossil spores and pollen) were established using Macphail and Cantrill (2006), Macphail (2007), Truswell and Macphail (2009), Daly et al. (2011), Kumaran et al. (2011), Raine et al. (2011), Bowman et al. (2014), and Macphail and Hill (2018).

2.3 Bioclimatic analysis

The nearest living relative (NLR) approach was used to estimate and reconstruct the mean annual temperature (MAT), warm mean month temperature (WMMT), cold mean month temperature (CMMT), and mean annual precipitation (MAP). The bioclimatic analysis used in this study involved all pollen and spore taxa that could be related to an NLR and are listed in Table 1. The NLR is a uniformitarian approach based on the assumption that climate tolerance of extant taxa can be extended into the past. However, factors such as misidentification of fossil taxa and/or their NLRs, unresolved differences in climate tolerance between fossil taxa and their NLRs, potentially incomplete climate tolerance of NLRs, and potential weakening of the connection between fossil taxa and NLRs through deep time may pose some concerns and need to be considered prior to the application of NLR-based climate reconstructions (Mosbrugger and Utescher, 1997; Mosbrugger, 1999; Pross et al., 2000; Utescher et al., 2000, 2014). Generally, these uncertainties and issues with the NLR approach increase when analysing plant remains or samples from deep-time geological records (Poole et al., 2005). To test the validity of our NLR-based climate estimates, we compare them to previously published independent botanical or geochemical proxies in the southern high latitudes spanning the late Eocene to early Oligocene (e.g. Colwyn and Hren, 2019; Houben et al., 2019; Korasidis et al., 2019; Bijl et al., 2021; Lauretano et al., 2021; Tibbett et al., 2021). Overall, these are generally in agreement and provide a certain level of confidence in the utility of the NLR-based climate estimates.

The NLR analysis in this study is combined with the probability density function (PDF). The PDF works by statistically constraining the most likely climate co-occurrence envelope for an assemblage (Harbert and Nixon, 2015; Hollis et al., 2019). Bioclimatic analysis was performed by using the *dismo* package in R (Hijmans et al., 2017) to cross-plot the modern distribution of the NLR from the Global Biodiversity Information Facility (GBIF; GBIF, 2021) with gridding from

https://doi.org/10.5194/cp-18-525-2022

Table 1. List of sporomorph taxa from the late Eocene to early Oligocene of ODP Site 1172, accompanied by botanical affinities, literature sources, nearest living relatives (NLRs) selected for climatic reconstruction, and inferred climate ranges from Macphail (2007).

Fossil taxon	Botanical affinity	Source	Selected NLR for climate analysis	Inferred climate range (Macphail, 2007)
Gymnosperms				
Araucariacites australis	Araucariaceae	Raine et al. (2011)	Araucariaceae	Lower to upper ?mesotherm
Dilwynites granulatus	Araucariaceae	Raine et al. (2011)	Araucariaceae	Lower to upper ?mesotherm
Dacrydiumites preacupressinoides	Podocarpaceae	Raine et al. (2011)	*Dacrydium cupressinum*	
Podocarpidites ellipticus	Podocarpaceae	Raine et al. (2011)	Podocarpaceae	Microtherm to ?megatherm
Podocarpidites spp.	Podocarpaceae	Truswell and Macphail (2009)	Podocarpaceae	Microtherm to ?megatherm
Dacrycarpites australiensis	Podocarpaceae	Truswell and Macphail (2009)	Podocarpaceae	Upper microtherm to lower mesotherm
Podocarpidites marwickii	Podocarpaceae	Raine et al. (2011)	Podocarpaceae	Microtherm to ?megatherm
Phyllocladidites mawsonii	*Lagarostrobos*	Raine et al. (2011)	*Lagarostrobos*	Upper microtherm to lower mesotherm
Phyllocladidites reticulasaccatus	Podocarpaceae	Raine et al. (2011)	Podocarpaceae	
Microcachryidites antarcticus	Podocarpaceae	Raine et al. (2011)	*Microcachrys*	Upper microtherm to lower mesotherm
Taxodiaceaepollenites hiatus	Cupressaceae	Raine et al. (2011)	Cupressaceae	
Microalatidites sp.	Podocarpaceae	Raine et al. (2011)	Podocarpaceae	Upper microtherm to lower mesotherm
Angiosperms				
Malvacipollis subtilis	Euphorbiaceae	Raine et al. (2011)	Euphorbiaceae	
Myricipites harrisii	Casuarinaceae	Raine et al. (2011), Macphail (2007)	*Gymnostoma*	Lower mesotherm to megatherm
Nothofagidites flemingii	*Nothofagus* subg. *Fuscospora*	Raine et al. (2011)	*Nothofagus* subg. *Fuscospora*	Upper microtherm to lower mesotherm
Nothofagidites spp.	*Nothofagus*	Raine et al. (2011)	*Nothofagus*	Upper microtherm to lower mesotherm
Nothofagidites emarcidus complex	*Nothofagus* subg. *Brassospora*	Truswell and Macphail (2009)	*Nothofagus* subg. *Brassospora*	Upper microtherm to lower mesotherm
Nothofagidites falcatus	*Nothofagus* subg. *Brassospora*	Raine et al. (2011)	*Nothofagus* subg. *Brassospora*	Upper microtherm to lower mesotherm
Nothofagidites lachlaniae complex	*Nothofagus* subg. *Fuscospora*	Raine et al. (2011)	*Nothofagus* subg. *Fuscospora*	Upper microtherm to lower mesotherm
Nothofagidites waipawaensis	*Nothofagus* subg. *Fuscospora*	Raine et al. (2011)	*Nothofagus* subg. *Fuscospora*	Upper microtherm to lower mesotherm
Nothofagidites asperus	*Nothofagus* subg. *Lophozonia*	Truswell and Macphail (2009)	*Nothofagus* subg. *Lophozonia*	Upper microtherm to lower mesotherm

https://doi.org/10.5194/cp-18-525-2022

Table 1. Continued.

Fossil taxon	Botanical affinity	Source	Selected NLR for climate analysis	Inferred climate range (Macphail, 2007)
Nothofagidites senectus	*Nothofagus*	Raine et al. (2011)	*Nothofagus*	
Nothofagidites brachyspinulosus	*Nothofagus* subg. *Fuscospora*	Raine et al. (2011)	*Nothofagus* subg. *Fuscospora*	
Proteacidites crassus	Proteaceae	Raine et al. (2011)	Proteaceae	Lower to upper mesotherm
Proteacidites pachypolus	Proteaceae	Macphail and Hill (2018)	Proteaceae	Lower to upper mesotherm
Proteacidites pseudomoides	Proteaceae	Raine et al. (2011)	*Carnarvonia*	Lower to upper mesotherm
Proteacidites leightonii	Proteaceae	Truswell and Macphail (2009)	Proteaceae	Lower to upper mesotherm
Proteacidites reticulatus	Proteaceae	Truswell and Macphail (2009), Raine et al. (2011)	Proteaceae	Lower to upper mesotherm
Proteacidites scaboratus	Proteaceae	Raine et al. (2011)	Proteaceae	Lower to upper mesotherm
Proteacidites similis	Proteaceae	Raine et al. (2011)	Proteaceae	Lower to upper mesotherm
Proteacidites parvus	Proteaceae	Bowman et al. (2014), Raine et al. (2011)	*Bellendena*	Lower to upper mesotherm
Periporopollenites polyoratus	Caryophyllaceae, Trimeniaceae	Raine et al. (2011)	Caryophyllaceae	
Parsonsidites psilatus	*Parsonsia*	Raine et al. (2011)	*Parsonsia*	
Spinizonocolpites sp.	Arecaceae	Raine et al. (2011), Kumaran et al. (2011)	Arecaceae	Upper mesotherm to megatherm
Tricolpites trioblatus	Scrophulariaceae, Convolvulaceae	Raine et al. (2011)	*Hebe*	Lower to upper mesotherm
Myrtaceidites cf. *parvus*	Myrtaceae	Raine et al. (2011)	Myrtaceae	
Malvacearumpollis mannanensis	Malvaceae	Raine et al. (2011)	Malvaceae	
Nupharipollis mortonensis	Araceae, Nymphaeaceae	Raine et al. (2011)	*Nuphar*	Upper mesotherm to megatherm
Sapotaceoidaepollenites cf *latizonatus*	Sapotaceae	Raine et al. (2011)	Sapotaceae	
Cryptogams				
Cyathidites australis	Cyatheaceae	Raine et al. (2011), Macphail et al. (1994)	Cyatheaceae	Upper microtherm to lower mesotherm
Cyathidites minor	Cyatheaceae	Raine et al. (2011)	Cyatheaceae	Upper microtherm to lower mesotherm

Table 1. Continued.

Fossil taxon	Botanical affinity	Source	Selected NLR for climate analysis	Inferred climate range (Macphail, 2007)
Cyathidites sp.	Cyatheaceae	Raine et al. (2011)	Cyatheaceae	Upper microtherm to lower mesotherm
Laevigatosporites ovatus	Blechnaceae	Raine et al. (2011), Truswell and Macphail (2009)	Blechnaceae	
Osmundacidites wellmanii	Osmundaceae	Raine et al. (2011)	*Todea*	
Osmundacidites sp.	Osmundaceae	Raine et al. (2011)	Osmundaceae	
Baculatisporites comaumensis	Osmundaceae, Hymenophyllaceae	Raine et al. (2011), Truswell and Macphail (2009), Macphail and Cantrill (2006)	*Hymenophyllum*	
Gleicheniidites senonicus	Gleicheniaceae	Truswell and Macphail (2009), Raine et al. (2011)	Gleicheniaceae	
Gleicheniidites spp.	Gleicheniaceae	Truswell and Macphail (2009)	Gleicheniaceae	
Dictyophyllidites arcuatus	Gleicheniaceae	Raine et al. (2011)	Gleicheniaceae	
Kuylisporites waterbolkii	Cyatheaceae	Raine et al. (2011)	Cyatheaceae	Upper microtherm to lower mesotherm
Clavifera rudis	Gleicheniaceae	Raine et al. (2011)	Gleicheniaceae	
Clavifera triplex	Gleicheniaceae	Raine et al. (2011), Truswell and Macphail (2009)	Gleicheniaceae	
Laevigatosporites major	Blechnaceae	Truswell and Macphail (2009), Raine et al. (2011), Macphail and Hill (2018)	Blechnaceae	
Stereisporites antiquasporites	Sphagnaceae	Truswell and Macphail (2009)	*Sphagnum*	± microtherm
Ceratosporites equalis	Selaginellaceae	Raine et al. (2011)	*Selaginella*	
Cibotiidites tuberculiformis	Schizaeaceae	Raine et al. (2011), Daly et al. (2011)	Schizaeaceae	
Polypodiisporites radiatus	Polypodiaceae	Raine et al. (2011)	Polypodiaceae	
Retriletes austroclavatidites	Lycopodiaceae	Raine et al. (2011)	*Lycopodium*	

https://doi.org/10.5194/cp-18-525-2022

the WorldCLIM climate surface (Fick and Hijmans, 2017). The datasets are then filtered to remove multiple entries per climate grid cell, plants whose botanical affinities are vague, doubtful, or redundant, and occurrences termed exotic (e.g. garden plants). Filtering was performed to avoid bias in the probability function that would likely lead to results leaning towards a particular location (Reichgelt et al., 2018). To test the robustness of the dataset, bootstrapping was applied, which was followed by the calculation of the likelihood of a taxon that occurs at a specific climate variable using the mean and standard deviation of the modern range of each taxon (Kühl et al., 2002; Willard et al., 2019). For a more detailed explanation of this method, see Willard et al. (2019) and Klages et al. (2020).

2.4 Quantitative and statistical analyses

Diversity indices (rarefaction, Shannon diversity index, equitability) were generated using the PAST statistical software (Hammer et al., 2001) with sample counts of ≥ 75 individuals. Rarefaction is an interpolation technique that is used to compare taxonomic diversity in samples of different sizes (Birks and Line, 1992; Birks et al., 2016). Rarefaction analyses using sample counts of ≥ 75 and ≥ 100 showed similar diversity trends. We, however, settled on counts with ≥ 75 individual grains because they offered an added advantage of filling in the gaps that would have been created if only samples with counts of ≥ 100 grains were used, thereby increasing the resolution of the studied section. The Shannon diversity index (H) is a measure of diversity that considers the number of individuals as well as the number of taxa and the evenness of the species present (Shannon, 1948). H ranges from 0 for vegetation communities with a single taxon to higher values where taxa are evenly distributed (Legendre and Legendre, 2012). Equitability (J), on the other hand, measures the level of abundance and how the species are distributed in an assemblage. Low J values indicate the dominance of a few species in the population (Hayek and Buzas, 2010).

Pollen zones (PZ) were defined following stratigraphically constrained analysis (CONISS; Grimm, 1987) in Tilia (version 2.6.1) using the total sum of squares with chord distance square-root transformation (Cavalli-Sforza and Edwards, 1967). In addition, we used detrended correspondence analysis (DCA; Hill and Gauch, 1980) sample scores to measure the sample-to-sample variance. DCA sample scores were generated using the *vegan* package (Oksanen et al., 2019) of the R statistical software (R Core Team, 2019).

3 Results

3.1 Palynological results from ODP Site 1172

The late Eocene–early Oligocene samples from the East Tasman Plateau (ODP Site 1172) yielded moderately to well-preserved sporomorphs. Eighty-one (81) individual sporomorph taxa were recorded from the 57 productive samples across the studied section. The sporomorph record is dominated by *Nothofagidites* spp., which makes up between 38 % to 48 % of all non-reworked sporomorphs across the studied interval (Fig. 2). *Podocarpidites* spp., *Myricipites harrisii*, *Cyathidites* spp., *Phyllocladidites mawsonii*, and *Araucariacites australis* form significant components of the palynoflora and occur with varying frequency (Fig. 2).

Based on results from rarefaction, the average diversity for the entire studied section was 20.1 ± 1.74 taxa per sample of 75 individuals. The sporomorph record based on CONISS is grouped into four pollen zones (PZ; Fig. 2), PZ 1 (early late Eocene; 37.97–37.52 Ma), PZ 2 (late Eocene–latest Eocene; 37.30–35.60 Ma), PZ 3 (latest Eocene–earliest Oligocene 35.50–33.36 Ma), and PZ 4 (earliest Oligocene; 33.25–33.06 Ma). All four zones consist of characteristic palynoflora assemblages that are described below. Taxa names in brackets refer to the NLRs.

3.1.1 Pollen zone 1 (37.97–37.52 Ma; 7 samples)

Pollen zone 1 is dominated by *Nothofagidites* spp. (*Nothofagus*), which accounts for ~ 48 % of all non-reworked palynomorphs. Taxa belonging to the *Brassospora* (~ 28 %) subgenus of *Nothofagus* make up the most abundant component, followed by *Fuscospora* (19 %) and *Lophozonia* (1 %), respectively. Other angiosperms (non-*Nothofagus*) on average account for 24 % of all sporomorphs. These are represented mainly, in order of decreasing occurrence, by *Myricipites harrisii* (*Gymnostoma*), *Proteacidites pseudomoides* (*Carnarvonia*), *Proteacidites* spp., *Spinizonocolpites* spp. (Arecaceae), *Malvacearumpollis mannanensis* (Malvaceae), and *Malvacipollis* spp. (Euphorbiaceae). The abundance of gymnosperms is generally low throughout PZ 1 and accounts for about 16 % of all non-reworked palynomorphs. These are also represented mainly, in order of decreasing occurrence, by *Podocarpidites* spp. (Podocarpaceae), *Phyllocladidites mawsonii* (*Lagarostrobos*), *Dacrydiumites praecupressinoides* (*Dacrydium*), and *Araucariacites australis* (Araucariaceae). Ferns and mosses account for about 12 % of the total sporomorphs and are represented by *Cyathidites* spp. (Cyatheaceae), *Dictyophyllidites* sp. (Gleicheniaceae), *Gleicheniidites* sp. (Gleicheniaceae), *Laevigatosporites* spp. (Blechnaceae), and *Stereisporites* sp. (*Sphagnum*).

Quantitatively, the sporomorph diversity for this zone, based on rarefied values, is 19.65 ± 1.32 species per sample of 75 individuals. With respect to the diversity indices, the yields for Shannon diversity (H) are between 2.33 and 2.69,

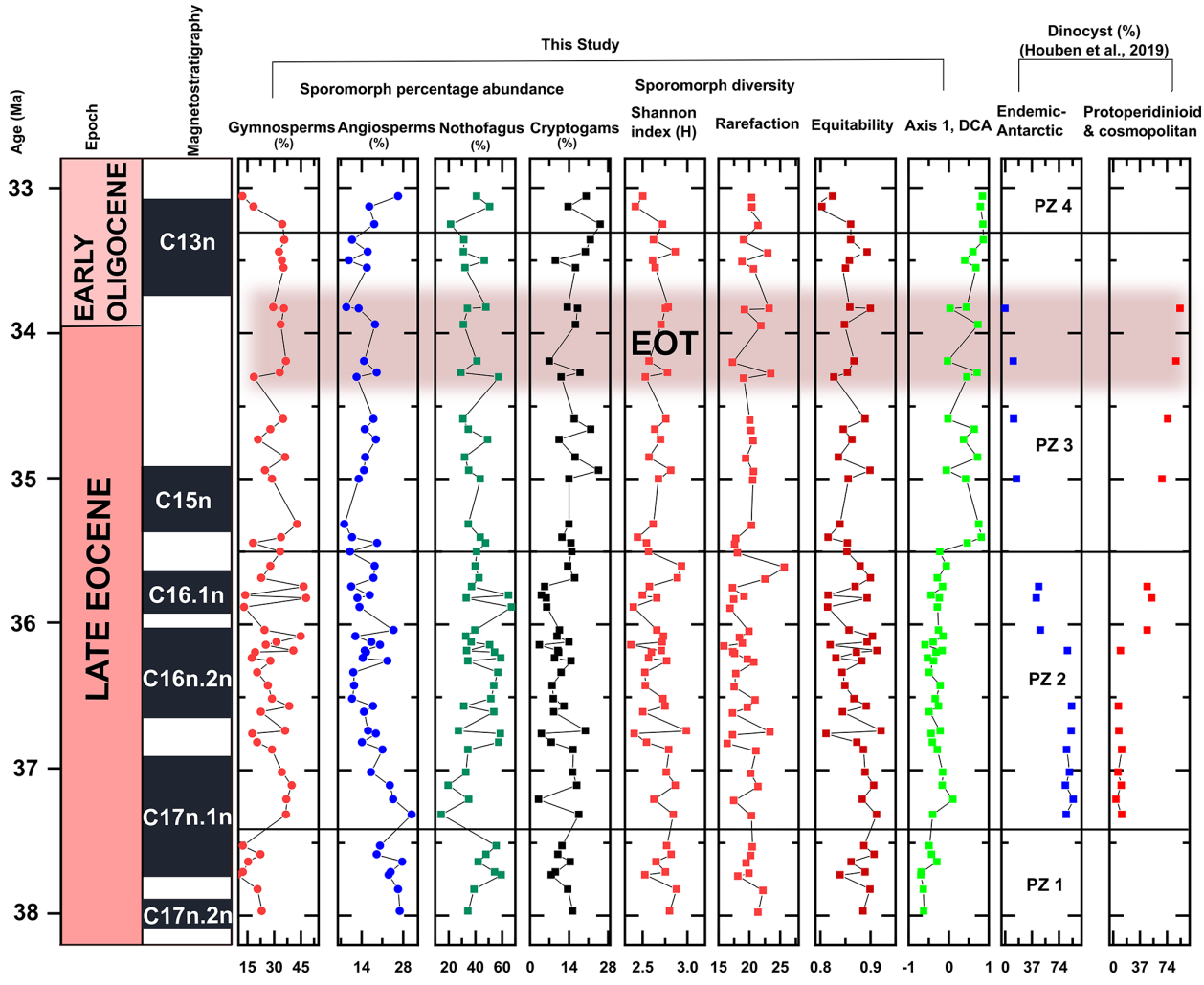

Figure 3. Sporomorph percentage abundances, diversity, and detrended correspondence analysis (DCA) results for ODP Site 1172. Percentage abundances for the major groups (gymnosperms, other angiosperms, *Nothofagus*, and cryptogams) are presented for all samples with pollen counts ≥ 75 grains. The DCA results are derived from the sample scores of axis 1 (which measures the sample-to sample variance) and show four distinct compositional groupings, as observed with CONISS, for the late Eocene–early Oligocene Site 1172 samples. Diversity is calculated based on Sander's rarefaction analysis with samples rarefied at 75 grains/individuals. Relative percentage abundances of Antarctic-endemic and protoperidinioid dinoflagellate cysts, the magnetostratigraphy, and the age model are after Houben et al. (2019).

Table 2. Summary of quantitative species diversity and DCA axis 1 sample scores between the late Eocene and early Oligocene from ODP Site 1172.

Analysis	Pollen zone 1		Pollen zone 2		Pollen zone 3		Pollen zone 4	
	Mean	(SD)	Mean	(SD)	Mean	(SD)	Mean	(SD)
Rarefaction (75 individuals)	19.65	1.32	19.44	2.49	20.15	1.79	21.16	1.37
Rarefaction (100 individuals)	22.29	1.87	21.78	2.85	22.52	2.31	23.75	1.32
Shannon index (H)	2.57	1.12	2.56	0.22	2.58	0.12	2.54	0.15
Equitability (J)	0.85	0.02	0.86	0.04	0.85	0.02	0.83	0.03
DCA (axis 1 sample scores)	−0.55	0.15	−0.29	0.15	0.44	0.33	0.83	0.03

averaging at 2.57 ± 1.12. Equitability (J) scores are set between 0.81 and 0.88, with an average of 0.85 ± 0.02 (Fig. 3; Table 2).

3.1.2 Pollen zone 2 (37.30–35.60 Ma; 27 samples)

PZ 2 sees the decline of *Nothofagidites* spp. to about 42 %. The *Brassospora* type remains the dominant *Nothofagus* subgenus, but with a substantial decline in abundance from about 28 % in PZ 1 to 22 % in PZ 2. The *Fuscospora* and *Lophozonia* subgenera, however, accounted for 19 % and 1 %, respectively (Fig. 2). In comparison to PZ 1, other angiosperms (non-*Nothofagus*) see a decline from about 24 % to 17 %. In order of decreasing abundance, the most significant taxa among non-*Nothofagus* angiosperms are *Myricipites harrisii* (*Gymnostoma*), *Proteacidites* spp. (Proteaceae), *Malvacearumpollis mannanensis* (Malvaceae), and *Malvacipollis* spp. (Euphorbiaceae). A sharp decline in *Proteacidites pseudomoides* (*Carnarvonia*) is coupled with the disappearance of *Spinizonocolpites* spp. (Arecaceae). Gymnosperms, on the other hand, almost double in relative abundance from about 16 % in PZ 1 to over 29 % in PZ 2. In order of decreasing abundance, gymnosperm taxa are dominated by *Podocarpus* spp. *Araucariacites australis* (Araucariaceae), *Dacrydiumites praecupressinoides* (*Dacrydium*), and *Phyllocladidites mawsonii* (*Lagarostrobos*). *Microcachryidites antarcticus* (*Microcachrys*) is a taxon that first appears in this zone and forms an important component (~ 11 %) of the gymnospermous assemblage. In addition to the above, cryptogams decline slightly in this zone, accounting for roughly 10 % of the total sporomorphs. The main members of this group are *Cyathidites* spp. (Cyatheaceae), *Gleicheniidites* (Gleicheniaceae), and *Laevigatosporites* spp. (Blechnaceae).

This zone has lower diversity than PZ 1. Based on rarefied values, the average diversity for PZ 2 is 19.44 ± 2.49 species per sample of 75 individuals. The results for the Shannon diversity index (H) are between 2.15 and 2.97, averaging at 2.56 ± 0.22. Equitability is set between 0.78 and 0.93, with an average of 0.86 ± 0.04 (Fig. 3; Table 2).

3.1.3 Pollen zone 3 (35.50–33.36 Ma; 20 samples)

Zone 3 shows a further decline in *Nothofagidites* spp. to ~ 38 %. However, the *Brassospora*-type *Nothofagus* sees a slight increase in abundance, while the *Fuscospora*-type *Nothofagus* declines sharply from the peak of 19 % observed in PZ 2 to 12 %. The *Lophozonia* type remains stable (~ 1 %). Other angiosperms (non-*Nothofagus*) see a slight decline and account for ~ 14 % of all non-reworked sporomorphs. These are represented mainly by *Myricipites harrisii* (*Gymnostoma*) and *Proteacidites* spp. (Proteaceae), *Malvacipollis* spp. (Euphorbiaceae), and *Malvacearumpollis mannanensis* (Malvaceae). Another important observation for this interval is the re-appearance of *Spinizonocolpites* spp. (Arecaceae) and *Proteacidites pseudomoides* (*Carnarvonia*). However, in contrast to PZ 1, *Spinizonocolpites* spp. are not consistently present. Gymnosperms increase slightly in this zone, accounting for ~ 31 %. The gymnosperms remain dominant with *Podocarpidites* spp. (Podocarpaceae). However, other important taxa such as *Araucariacites australis* (Araucariaceae), *Phyllocladidites mawsonii* (*Lagarostrobos*), and *Microcachryidites* (*Microcachrys*) decline. *Dacrydiumites praecupressinoides* (*Dacrydium*) reaches its peak abundance in this zone. Cryptogams significantly increase in abundance and are represented, in order of abundance, by *Cyathidites* spp. (Cyatheaceae), *Laevigatosporites* spp. (Blechnaceae), *Osmundacidites* (Osmundaceae), *Polypodiisporites radiatus* (Polypodiaceae), and *Clavifera* spp. (Gleicheniaceae).

Based on rarefied values, the average diversity for this PZ is 20.15 ± 1.79 species per sample. The results for Shannon diversity (H) are between 2.37 and 2.80, averaging at 2.58 ± 0.12. Equitability (J) is set between 0.81–0.91, averaging at 0.85 ± 0.02 (Fig. 3; Table 2).

3.1.4 Pollen zone 4 (33.25–33.06 Ma; 3 samples)

The percentage abundances of *Nothofagidites* spp. (*Nothofagus*), including *Brassospora* (~ 23 %), *Fuscospora* (12 %), and *Lophozonia* types, remain unchanged, whereas other angiosperm percentages increase substantially from 14 % in PZ 3 to ~ 20 %. In order of decreasing abundance, these are represented by *Myricipites harrisii* (*Gymnostoma*) and *Proteacidites pseudomoides* (*Carnarvonia*). PZ 4 also sees the emergence of new angiosperms such as *Sapotaceoidaepollenites* cf. *latizonatus* (Sapotaceae) and *Parsonsidites psilatus* (*Parsonsia*). Gymnosperms, however, see a sharp decline in this interval, accounting for about 21 % of the total sporomorph taxa, with *Podocarpidites* spp. (Podocarpaceae) and *Dacrydium praecupressinoides* (*Dacrydium*) as the main components. *Microcachryidites antarcticus* (*Microcachrys*), *Araucariacites australis* (Araucariaceae), and *Phyllocladidites mawsonii* (*Lagarostrobos*) show significant declines, whereas cryptogams increase to ~ 20 %. The cryptogams are represented, in order of decreasing abundance, by *Cyathidites* spp. (Cyatheaceae), *Laevigatosporites* spp. (Blechnaceae), *Dictyophyllidites* sp. (Gleicheniaceae), and *Cibotiidites tuberculiformis* (Schizaeaceae).

Average diversity (21.16 ± 1.37 species per sample) is slightly higher than in PZ 3. The results for Shannon diversity (H) are between 2.42 and 2.72, averaging at 2.54 ± 0.15. Equitability (J) is set between 0.80–0.87, averaging at 0.83 ± 0.03 (Fig. 3; Table 2).

4 Discussion

4.1 Vegetation composition and altitudinal zonation

Throughout the studied section, abundant *Nothofagidites* spp. and common *Podocarpidites* spp. *Myricipites har-*

risii and *Phyllocladidites mawsonii* indicate the presence of *Nothofagus*-dominated temperate rainforest (Truswell and Macphail, 2009; Bowman et al., 2014), which likely grew across lowland and mid-altitude elevations in eastern Tasmania. The occurrence of *Araucariacites australis*, *Microcachryidites antarcticus*, and *Proteacidites parvus* may also suggest that a component of the sporomorph assemblage reflects higher altitudes with more open forest conditions (Macphail, 1999; Kershaw and Wagstaff, 2001). In addition, pollen taxa belonging to *Arecaceae*, *Gymnostoma*, and *Carnarvonia* indicate the existence of a paratropical vegetation community that grew in sheltered lowland and coastal areas (Huurdeman et al., 2021). The paratropical rainforest likely occupied lowlands and coastal areas, while temperate rainforest likely grew at higher elevations, similar to vegetation communities that prevailed on Wilkes Land and Tasmania during the early to mid-Eocene (Pross et al., 2012; Contreras et al., 2013, 2014). The existence of different vegetation communities with NLRs that currently grow at different temperatures and elevations suggests that vegetation across eastern Tasmania were subject to climatic gradients related to differences in elevation and/or distance to the coastline. This is supported by reports of a topographic divide between sites facing the cool Tasman Current (Gippsland basin, eastern Tasmania) and the westerly located south Australian basins (Holdgate et al., 2017), which may have served as the locations for higher-altitude temperate forest taxa. The following sub-sections further describe each of these vegetation communities in detail.

4.1.1 Lowland to mid-altitude *Nothofagus–Podocarpus* rainforest

Abundant *Nothofagidites* spp. and common *Podocarpidites* spp., *Myricipites harrisii*, *Phyllocladidites mawsonii*, and Cyatheaceae give an indication of a lowland to mid-altitude *Nothofagus–Podocarpus*-dominated rainforest thriving under high-precipitation regimes (MAP $> 1300\,\mathrm{mm\,yr^{-1}}$) in Tasmania during the late Eocene to the earliest Oligocene. The main canopy is primarily made up of *Nothofagidites* spp. (*Nothofagus*/southern beech) and podocarps (*Dacrydiumites, Podocarpidites, Dacrycarpites*) with rare Cupressaceae trees. Southern beech forests can either occur as pure stands or a mixed forest, making the definition and recognition of regional or local forest types from fossil pollen and spores challenging. Today, pure beech stands in New Zealand are mostly montane to subalpine, and lowland mixed beech forests are associated with diverse broadleaf angiosperms and canopy-emergent gymnosperms (Ogden et al., 1996). Following Dettmann et al. (1990), we categorize *Nothofagidites* pollen taxa into the subgenera *Brassospora*, *Fuscospora*, and *Lophozonia*. Extant *Fuscospora* and *Lophozonia* types thrive in cool-temperate conditions in Tasmania, southeastern Australia, New Zealand, and southern South America (Hill, 1994, 2017; Veblen et al., 1996; Read et al., 2005), while the *Brassospora* type are today restricted to warm-temperate–subtropical conditions in New Guinea and New Caledonia (Hill and Dettmann, 1996; Veblen et al., 1996). These Brassospora-type *Nothofagus* grow today at lower to mid-altitudes that receive high and consistent rainfall, but also in montane and subalpine areas (typically above 500 m), pointing to their wide ecological and climate tolerance (MAT: 10.6 to 23.5 °C; Read et al., 2005).

Myricipites harrisii (Casuarinaceae) has two potential NLRs, *Casuarina/Allocasuarina* and *Gymnostoma*. *Casuarina/Allocasuarina* have xeromorphic features indicating adaptation to an arid climate with frequent fires (Hill, 2017; Lee et al., 2016; Hill et al., 2020). We selected the rainforest clade *Gymnostoma* as the most likely NLR of our fossil taxon *Myricipites harrisii*, based on the subtropical affinities of the associated palynoflora. This is also supported by Paleogene vegetation reconstruction for southeastern Australia based on macrofossil remains, which indicates rainforest communities (Christophel et al., 1987; Macphail et al., 1994; Hill, 2017), with *Gymnostoma* being common from the Paleocene to Oligocene and later being replaced by *Casuarina/Allocasuarina* (sclerophyll taxa) in the Miocene (Evi et al., 1995; Boland et al., 2006; Holdgate et al., 2017; Hill et al., 2020).

Dacrydium cupressinum is suggested as the most likely NLR of *Dacrydiumites praecupressinoides* (rimu; Raine et al., 2011). Today, *Dacrydium cupressinum* occurs as a minor component in the kauri forest of Northland, New Zealand and as emergent taxa commonly associated with *Agathis australis* (Araucariaceae) and *Podocarpus totara* (Farjon, 2010). The NLR of *Phyllocladidites mawsonii*, *Lagarostrobos franklinii* (Tasmanian Huon pine; Raine et al., 2011), is very abundant at Site 1172. *Lagarostrobos* are evergreen cool-temperate riparian trees that grow in Tasmania close to riverbanks (Farjon, 2010; Hill, 1994, 2017). Apart from forming groves that mark stream courses at low altitudes (Hill and Macphail, 1983; Farjon, 2010), they may also be found away from water courses on wet hillsides in temperate forest (Farjon, 2010; Bowman et al., 2014). *Lagarostrobos* is one of the most common gymnosperms at ODP Site 1172, and its percentage abundance is similar to those recovered from wells offshore Gippsland Basin (the Gropper-1, Mullet-1, and Bluebone-1 wells; Partridge, 2006). *Lagarostrobos* occurs with even higher percentages in the Middle *Nothofagidites asperus* Zone of the terrestrial record of the Gippsland Basin, where it appears to be overrepresented (Holdgate et al., 2017).

The two possible NLR relatives for *Proteacidites pseudomoides* are *Carnarvonia* and *Lomatia*. *Carnarvonia* thrives in warm-temperate to paratropical areas such as wet northeastern Australia (Mabberley, 1997; Cooper and Cooper, 2004) and grows into large trees (Hyland, 1995). *Lomatia* grows as shrubs and small trees in remnant gallery warm-temperate rainforests, for example along creek lines on sandstones in Northern Sydney (Bowman et al., 2014; Myer-

scough et al., 2007). *Carnarvonia* was selected as the likely NLR relative because it significantly increases in intervals where warmth-loving taxa such as Arecaceae, *Brassospora*-type *Nothofagus*, Gleicheniaceae, and Cyatheaceae thrive.

4.1.2 High-altitude temperate rainforest and shrubland

Components of the palynoflora that reflect higher-altitude and more open vegetation on soils with low fertility are *Araucariacites australis*, *Proteacidites parvus*, and *Microcachryidites antarcticus* (Kershaw and Wagstaff, 2001; Macphail et al., 1999). Today, Araucariaceae trees grow in cool-temperate forests in Chile and Argentina and extend to the tree line (Veblen et al., 1996; Sanguinetti and Kitzberger, 2008). In the Andes, trees belonging to Araucariaceae are found at altitudes of 600–800 m a.s.l., receive high amounts of annual rainfall (2000–3000 mm yr^{-1}), and experience hot and dry spells in summer (Farjon, 2010). Araucariaceae build pure stands at higher altitudes or mixed Valdivian rainforest at lower altitudes (Farjon, 2010). Increases in araucarian sporomorph taxa between 37.30–35.60 Ma in Tasmania give an indication of a dense, emergent cover of Araucariaceae thriving in relatively dry environments (Kershaw and Wagstaff, 2001). *Microcachrys* (Raine et al., 2011), the nearest living relative of *Microcachryidites antarcticus*, is a creeping shrub that grows in alpine/subalpine areas and is today restricted to western Tasmania under boreal to cool-temperate conditions (Truswell and Macphail, 2009; Biffin et al., 2012; Carpenter et al., 2011). Therefore, increases in this Tasmanian endemic alpine shrub (*Microcachrys*) from 37.30 to 35.60 Ma, together with *Bellendena* (a low-growing protea shrub; NLR of *Proteacidites parvus*), and Araucariaceae (emergent canopy), suggest that the vegetation that thrived at higher altitudes in Tasmania preferred cool-temperate conditions.

4.2 Subtropical vegetation and early late Eocene cooling from 37.97 to 35.60 Ma

Throughout PZ 1 (37.97–37.52 Ma), abundant *Nothofagus* (especially the *N. brassii* type) with secondary Podocarpaceae and *Gymnostoma* and minor Arecaceae, *Carnarvonia*, and cryptogams suggest the presence of a temperate *Nothofagus*-dominated rainforest with subtropical elements. Sporomorph-based climate estimates indicate these forests grew under a MAT of 14.2–15.1 °C and a MAP of 1467–1681 mm yr^{-1} (Fig. 4). The vegetation-based summer temperature reconstructions of ca. 18.5 °C closely corroborate the brGDGT-biomarker reconstructions from the same site (Bijl et al., 2021), supporting the notion of a potential seasonal bias of this palaeothermometer (Contreras et al., 2014; Naafs et al., 2017). The warmth-loving taxa formed the main lowland forest components occupying sheltered areas and lowland subtropical coastal zones (Dowe, 2010; Carpenter et al., 2012; Tripathi and Srivastava, 2012; Verma et al., 2020)

and swamps (Kershaw, 1988). Sporomorph-based temperature estimates yield a cold month mean temperature (CMMT) of well above freezing (11.2–12.5 °C; Fig. 4). The decline and, to a large extent, the absence of cool-temperate taxa, coupled with persistent warm-temperate (12–17 °C; Emanuel et al., 1985) to subtropical (17–24 °C; Emanuel et al., 1985) taxa, further point to the expansion of warm-temperate–paratropical rainforest up into the mid-altitudes and uplands.

The *Nothofagus*-dominated rainforest continued into PZ 2 (37.30–35.60 Ma). However, at ∼ 37.30 Ma, a distinct environmental change occurred, leading to a drop in, and in some instances the demise of, warm-temperate and subtropical taxa (*Nothofagus* subgenus *Brassospora*, *Carnarvonia*, Arecaceae; Fig. 2). This vegetation change continued throughout PZ 2, along with a concomitant rise in the relative abundances of *Lagarostrobos* and *Microcachrys* and a decline in diversity (Table 2) ∼ 3 Ma prior to the EOT. The increased occurrence of microthermal taxa points to a cool-temperate (southern beech)-dominated rainforest with secondary Podocarpaceae expanding into lowland regions previously occupied by mesothermal taxa. The late Eocene cool-temperate *Nothofagus*–Podocarpaceae-dominated rainforest has been suggested to resemble the modern Valdivian rainforest of Chile (Veblen, 1982; Cantrill and Poole, 2012; Bowman et al., 2014) and the cool-temperate *Nothofagus*-dominated rainforest with riparian *Lagarostrobos* restricted to river gullies in Victoria, Australia (Read and Hill, 1985) or on fertile soils in lowland Tasmania (Read and Hill, 1985; Macphail, 2007; Francis et al., 2008).

This interpretation is reflected in our sporomorph-based MAT estimates indicating a 2–3 °C decline in MAT (Fig. 4). Our findings also corroborate previous late Eocene studies throughout Australia indicating an increase in *Nothofagus* subgenus *Fuscospora* along with a substantial decline in *Brassospora*-type *Nothofagus* and the demise of most Proteaceae, Arecaceae, and most Australian angiosperms (Kemp, 1978; Kershaw, 1988; Christophel and Greenwood, 1989; Truswell, 1993; Martin, 1994, 2006; Macphail et al., 1994; Partridge and Dettmann, 2003; Korasidis et al., 2019). In line with the vegetation change, biomarker-based reconstruction from Site 1172 also indicates that SSTs decline by ca. 2–3 °C starting around 37.5 Ma (Fig. 4). However, the cooling indicated by both independent proxies is not reflected in the lipid-biomarker-based terrestrial MAT estimates, and the reason for this disparate trend remains unknown.

The transition from a warm-temperate rainforest with paratropical elements to cool-temperate forests in the Tasmanian Gateway region also matches an early late Eocene (37.3 Ma) cooling in the Southern Ocean (Kerguelen Plateau) ∼ 3 Myr prior to the EOT (Villa et al., 2008, 2014; Scher et al., 2014). The 2–3 °C sporomorph-based MAT (100–200 kyr) cooling around 37.3 Ma coincides with a regional

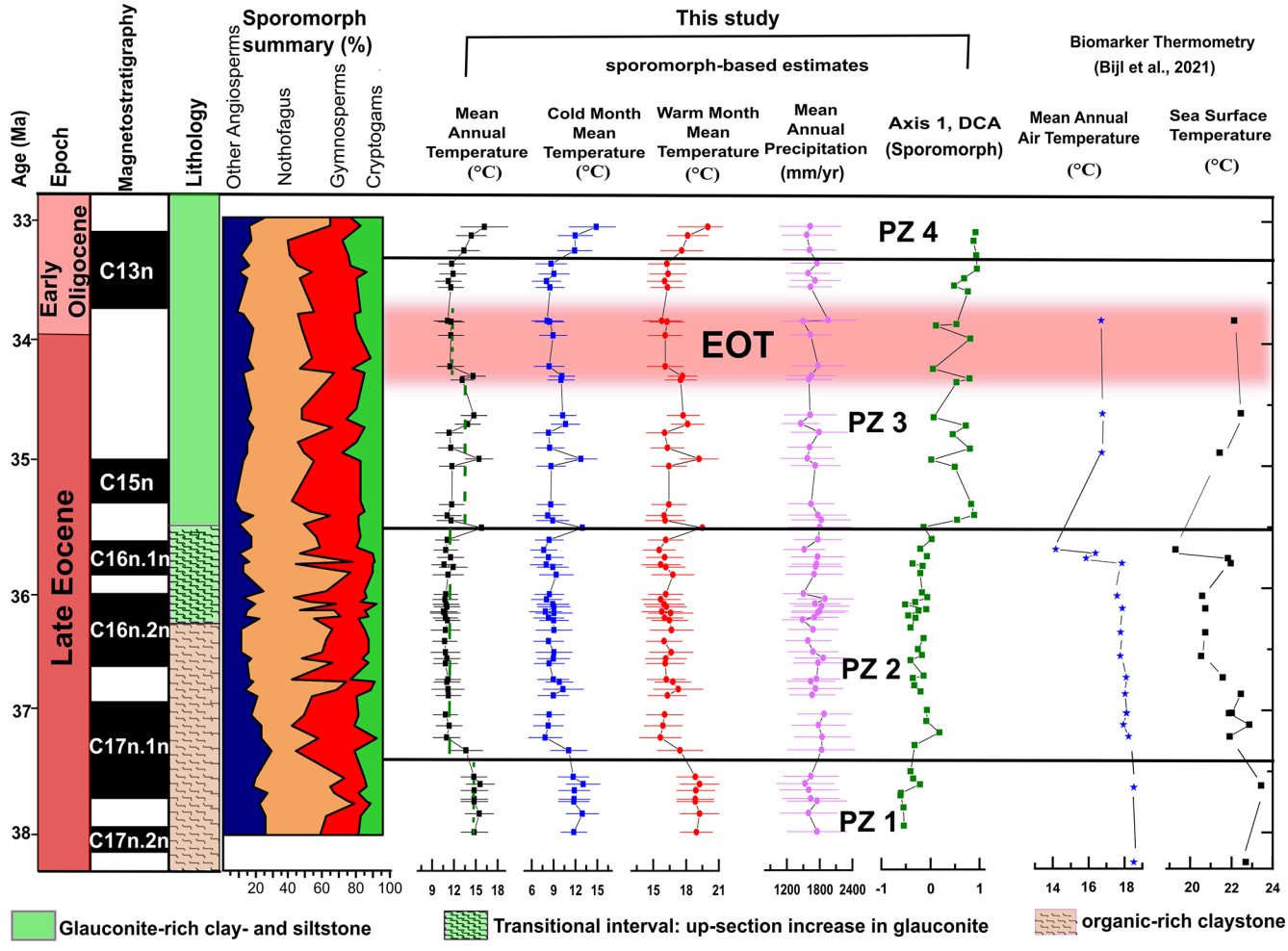

Figure 4. Comparison of our sporomorph-based climate estimates, $MAAT_{soil}$ values based on MBT'5me, TEX_{86}-based SSTs, and sample scores for DCA axis 1 from the late Eocene to early Oligocene of ODP Site 1172. Sporomorph-based estimates are based on the use of the nearest living relative (NLR) and probability density function (PDF). The range of each climate estimate represents the mathematical error and not the real range, and may have been a result of uncertainties associated with the use of the NLR approach. Broken green lines indicate average temperatures for sporomorph-based MATs. Biomarker thermometry data are from Bijl et al. (2021). The ~ 790 kyr interval corresponding to the EOT (34.44–33.65 Ma; Hutchinson et al., 2021) is indicated by the horizontal pink bar. The age model is after Houben et al. (2019).

transient (~ 140 kyr) cooling event at ODP Site 738 (Kerguelen Plateau) known as the Priabonian Oxygen Maximum (PrOM; Scher et al., 2014). The PrOM event, placed within magnetochron C17n.1n of the late Eocene, points to the temporary growth of ice sheets on East Antarctica based on a positive excursion of benthic $\delta^{18}O$ (Scher et al., 2014). However, on the Kerguelen Plateau, differences in neodymium isotopic composition (ε_{Nd}) between bottom waters and terrigenous sediments point to changes in sediment provenance as opposed to changes in the reorganization of ocean currents (Scher et al., 2014). The transient 2–3 °C sporomorph-based MAT cooling phase is followed by a period with a sustained cooler climate from 37.2 to 35.6 Ma (Fig. 4). This sustained cooler climate may have caused the climate threshold of the frost-sensitive (subtropical) taxa to be exceeded, hence their continued decline and demise. In the marine realm, Antarctic-endemic dinoflagellate cysts (e.g. *Deflandrea antarctica*, *Vozzhennikovia* spp., and *Enneadocysta dictyostila*) become dominant at Site 1172 (Fig. 3; Stickley et al., 2004; Houben et al., 2019). The dominant Antarctic-endemic dinocysts in addition to general sea surface circulation models (Huber et al., 2004) point to the East Tasman Plateau and east Tasmania being bathed by relatively cool Antarctic-derived surface waters (Houben et al., 2019), which is consistent with TEX_{86}-based sea surface temperature records (~ 3–4 °C cooling; Houben et al., 2019; Bijl et al., 2021). Regionally, this sustained cool-temperate terrestrial MAT matches with oligotrophic conditions associated with low nutrients, stratification of the water mass, and increased efficiency of the ocean's biological pump, which

favoured cooling as a result of carbon being sequestered from surface water in the Southern Ocean (Villa et al., 2008, 2014).

Close to the top of PZ 2 (35.7 Ma; Fig. 4), branched GDGT(glycerol dialkyl glycerol tetraether)-based MATs and SSTs show strong and rapid cooling, which is not mirrored by the pollen-based climate estimates. However, strong fluctuations in gymnosperms and an increase in cryptogams (Figs. 2 and 3) and diversity towards the top of PZ 2 indicate increasing environmental disturbance, which might be linked to the recorded change in lipid biomarker-based MATs. The rapid cooling most likely created gaps within the canopy, triggering an expansion of cryptogams. The divergence between the different proxy signals could be related to their different origins and transport mechanisms. Whereas the lipid biomarkers are strongly controlled by the depositional settings, including the river run-off, and the tectonic and geographic evolution (Bijl et al., 2021), the terrestrial palynological signal mainly consists of wind-dispersed pollen and spores. The long distance between the study site (ODP Site 1172) and mainland Tasmania (more than 100 km) in the Eocene makes a major influence of river/water-transported sporomorphs unlikely.

4.3 Warm- and cold-temperate terrestrial climate fluctuation from 35.50–34.59 Ma

PZ 3 (35.50–33.36 Ma) is characterized by a major shift in sporomorph assemblages, represented by an increase in *Podocarpus*, declines in *Lagarostrobos*, *Microcachrys*, Araucariaceae, and *Fusca*-type *Nothofagus*, along with the re-emergence of subtropical and warm-temperate taxa. The peak in tree ferns, especially Cyatheaceae, indicate a period of disturbance (Vajda et al., 2001) within this interval of vegetation shift. However, we are not able to attribute the disturbance within this period (35.50–34.59 Ma) to an increase in fire frequencies as there is an absence of charcoal particles within our records. Sporomorph-based temperature reconstructions indicate several fluctuations between warm and cool climate phases with MATs between 10.6 and 15.3 °C (Fig. 4). In the regional Australo-Antarctic area, a similar phase of warming and cooling is observed in the late Eocene (35.8–34.7 Ma) climate records of Prydz Bay (Passchier et al., 2017; Tibbett et al., 2021) and southern Australia (Benbow et al., 1995). Again, pollen-based WMMTs at Site 1172 closely match lipid-biomarker-derived MATs (Fig. 4). In comparison, our sporomorph-based warm and cool climate fluctuation phase between 35.50 to 34.59 Ma is recorded as a recovery phase in the lipid-biomarker-based MAT reconstruction. The fluctuations of pollen-based temperature estimates may be at least partly caused by the proxy method, which relies on presence–absence data. However, a more detailed proxy comparison is hampered by the relatively low resolution of the lipid biomarker in PZ 3.

Expansions and restrictions of cool-temperate and warm-temperate forests, which indicate cooling and warming phases, are consistent with previous late Eocene geochemical, sedimentological, and palynological studies reporting an increase in sea surface temperature (TEX_{86}-based SST; Houben et al., 2019; Bijl et al., 2021), widespread deposition of glauconite (Stickley et al., 2004), and increases in cosmopolitan and protoperidinioid dinocysts (Fig. 3; Stickley et al., 2004; Houben et al., 2019; Bijl et al., 2021). Though the glauconitic unit is interpreted as marking deepening and current inception due to a widening of the Tasmanian Gateway (Stickley et al., 2004), a more recent counterargument links the deposition of the greensand to atmospherically forced invigorated circulation in the Southern Ocean, which helped to prepare Antarctica for rapid expansion of ice (Houben et al., 2019) and a further circulation change $\sim$2 Ma later (at the EOT). However, in addressing the deposition of greensands along the south Australian margin, ocean model studies (Baatsen et al., 2016) point to a further expansion of the eastward throughflow into the southwest Pacific Ocean. Our sporomorph-based MAT consequently showed an average 2 °C rise in temperature between 35.50 and 34.59 Ma, coinciding with earlier reports of the initial deepening of the Tasmanian Gateway (Stickley et al., 2004). This is further supported by the common appearance of low-latitude cosmopolitan dinoflagellate cyst taxa that, rather than being supplied by the East Australian Current, are reported to have been sourced from the throughflow associated with the eastward proto-Leeuwin Current (Huber et al., 2004; Stickley et al., 2004; Houben et al., 2019). These events, coupled with an $\sim$2 °C recovery in SSTs (TEX_{86}-based; Houben et al., 2019; Bijl et al., 2021) between 35.7 and 34.59 Ma, most likely point to an influence of warm surface waters associated with the Australo-Antarctic Gulf (AAG) at ODP Site 1172 (Houben et al., 2019), which is reported to have been close to land (eastern Tasmania; Stickley et al., 2004) at that time, thereby affecting the terrestrial climate and vegetation.

4.4 EOT cooling and climate rebound in the earliest Oligocene from 34.30 to 33.06 Ma

At the onset of the EOT, our sporomorph record provides evidence for a return to a sustained cooler period spanning 34.30 to 33.82 Ma in Tasmania. This EOT cool phase coincides with the demise of *Spinizonocolpites* sp. (Arecaceae), a drop in Cyatheaceae and Gleicheniaceae, and slight increases in *Microcachrys* and *Lagarostrobos*. The palynoflora assemblage during the EOT is further characterized by a drop in overall angiosperm (non-*Nothofagus*) diversity, with gymnosperms and *Nothofagus* (*Brassospora* type) being common and co-dominating. Previous studies in southeast Australia (e.g. Macphail et al., 1994; Benbow et al., 1995; Holdgate et al., 2017; Lauretano et al., 2021) record a contemporaneous drop in angiosperm diversity and the final demise of Arecaceae (thermophilous elements) at the end of the Eocene

(Pole and Macphail, 1996; Martin, 2006). Quantitatively, our sporomorph-based MAT reconstruction records an ∼2 °C decline across the EOT (Fig. 4), which coincides with ∼2.4 and 5 °C cooling steps in southeastern Australia (MBT'5me-based MAATsoil; Lauretano et al., 2021) and East Antarctica (Prydz Bay; MBT'5me-based MAATsoil; Tibbett et al., 2021), respectively. This cooling in our terrestrial record further matches the principal geochemical signature of EOT in the marine realm: the ∼ +1.5 ‰ excursion of the oxygen isotope ratio of deep-sea benthic foraminifera (Zachos et al., 1996; Coxall et al., 2005; Pälike et al., 2006; De Vleeschouwer et al., 2017; Fig. 5) associated with global cooling (Zanazzi et al., 2007; Pearson et al., 2009; Pagani et al., 2011; Hutchinson et al., 2021; Tibbett et al., 2021). This cooling at the EOT has been linked to a global decline in atmospheric pCO_2 (Pearson et al., 2009; Lauretano et al., 2021).

Between ∼33.25 and 33.06 Ma (PZ 4), the sporomorph-based climate estimates indicate a warming, with MATs between 12.7 and 15.3 °C (Fig. 4). In addition, the presence of warmth-loving taxa, notably Sapotaceae, *Parsonsia* (Silkpod), and Polypodiaceae (subtropical epiphytes), further indicate a warming phase. The pollen flora resembles Oligocene warm-temperate *brassii* southern-beech-dominated forests of Karamu in the Waikato Coal Measures of New Zealand (Pocknall, 1985). The increase in *brassii*-type *Nothofagus* coupled with the appearance of Sapotaceae and subtropical epiphytes suggests that, at least locally on lowlands, eastern Tasmania was warm enough to accommodate warm-temperate vegetation in the earliest Oligocene. Previous earliest Oligocene studies in southeast Australia (Korasidis et al., 2019) show the presence of a cool-temperate rainforest community. The palynoflora on east Antarctica (Askin, 2000; Askin and Raine, 2000; Prebble et al., 2006; Tibbett et al., 2021) and northeast Tasmania (Hill and Macphail, 1983) suggest an early Oligocene cold-temperate *Nothofagus* (subgenus *Lophozonia* or *Fuscospora*)–Podocarpaceae vegetation. These palynoflora of northern Tasmania and east Antarctica are, however, reported to have most likely been made up of prostrate deciduous dwarf trees or small-stature closed southern beech/podocarp refugia with a vegetation community that likely struggled to survive (Askin, 2000; Askin and Raine, 2000; Prebble et al., 2006; Francis et al., 2008; Tibbett et al., 2021). However, rather than a regional scrub (e.g. in Antarctica), the slight increase in angiosperms (other than *Nothofagus*) and cryptogams point to a local warm-temperate forest growing along eastern Tasmania in the earliest Oligocene. Today, temperate forests in New Zealand and Tasmania host a diverse range of cryptogams, as compared to scrub communities that do not offer other taxa to thrive under the low, closed canopies (Prebble et al., 2006).

The terrestrial cooling observed across the EOT followed by a rapid recovery in the earliest Oligocene matches a partial return to warmer temperatures seen in previously reported terrestrial (Colwyn and Hren, 2019; Lauretano et al., 2021) and marine studies (Katz et al., 2008; Lear et al., 2008; Liu et al., 2009; Houben et al., 2012). The synchroneity between terrestrial and marine records suggests that, in addition to localized events (sustained Tasmanian Gateway deepening and widening; Stickley et al., 2004), the EOT and earliest Oligocene ETP record may also be responding to a much wider regional or global event. The most common explanation for the global cooling (Zanazzi et al., 2007; Pagani et al., 2011; Hutchinson et al., 2021; Tibbett et al., 2021) across the EOT and the transient warming in the earliest Oligocene is the decline in concentration of atmospheric carbon dioxide (pCO_2) and its recovery or rebound in the earliest Oligocene, respectively (Pearson et al., 2009; Heureux and Rickaby, 2015; Anagnostou et al., 2016; Fig. 5). Our results suggest that the warming, or at least the lack of sustained cooling following the EOT in eastern Tasmania, may be related to a combination of the pCO_2 recovery (Pearson et al., 2009) and sustained Tasmanian Gateway deepening and widening (Stickley et al., 2004; Houben et al., 2019), allowing the influx of more warm surface waters from the AAG into the southwest Pacific, thereby affecting the terrestrial climate and vegetation along eastern Tasmania.

5 Conclusions

The late Eocene–early Oligocene vegetation reconstructed from terrestrial palynomorphs recovered from ODP Site 1172 (East Tasman Plateau) is characterized by three major climate transitions.

The early late Eocene sporomorph record suggests a distinct 2–3 °C terrestrial cooling at 37.30 Ma coupled with a transition from a warm-temperate *Nothofagus*–Podocarpaceae-dominated rainforest with paratropical elements to a cool-temperate *Nothofagus*-dominated rainforest with secondary Podocarpaceae. This terrestrial cooling at 37.30 Ma and sustained cool climate from 37.2–35.60 Ma coincides with a long-term SST decline from ∼23 to 19 °C at ODP Site 1172, a regional transient cooling event (PrOM) at ODP Site 738 (Kerguelen Plateau; Scher et al., 2014), and a relatively long-term regional Southern Ocean cooling due to carbon being sequestered from surface water (Villa et al., 2008, 2014).

The expansion and restriction of cool- and warm-temperate forests from 35.5 to 34.49 Ma were followed by a period of cooling across the EOT (34.30–33.82 Ma). The terrestrial climate fluctuation in this zone is consistent with latest-Eocene geochemical, sedimentological, and palynological studies that report an increase in SST, a recovery in MBT'5me-based MAATsoil (biomarker thermometry), widespread deposition of glauconite, and the common occurrence of low-latitude cosmopolitan and protoperidinioid dinocysts. These are interpreted as being linked to the initial deepening of the Tasmanian Gateway, paving the way for

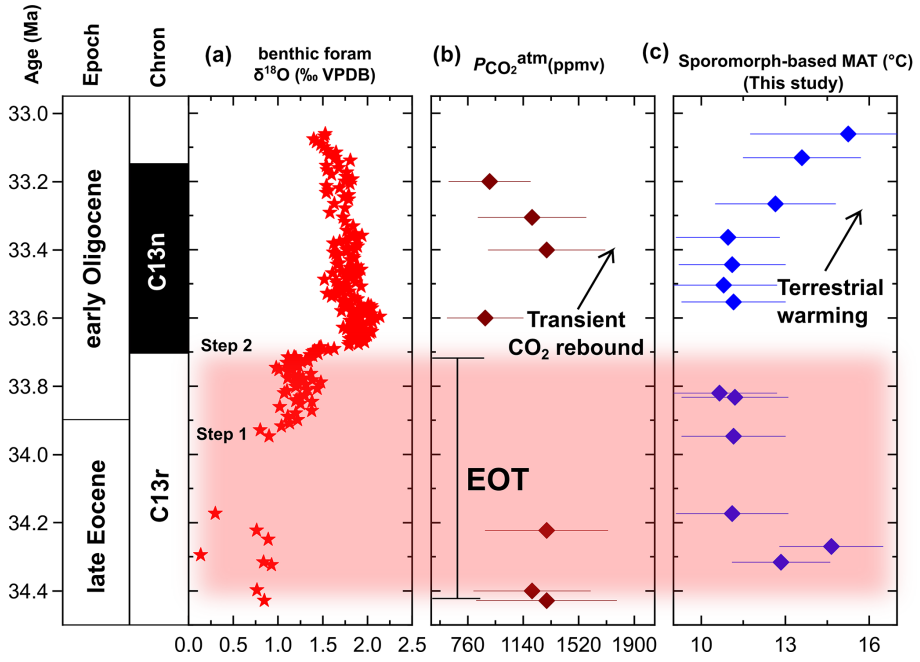

Figure 5. Comparison of the sporomorph-based MAT in the Tasmanian Gateway region across the EOT and earliest Oligocene to regional and global marine EOT and earliest Oligocene records. **(a)** Marine benthic foraminiferal calcite δ^{18}O record from ODP Site 1218 (Pälike et al., 2006). **(b)** Marine δ^{11}B-derived atmospheric pCO$_2$ record (Anagnostou et al., 2016). **(c)** Terrestrial temperature change across the EOT and earliest Oligocene based on our sporomorph-based MATs from ODP Site 1172.

the warm water associated with the PLC to affect both the terrestrial and the marine climate in this region.

The post-EOT (earliest Oligocene) recovery was characterized by a warm-temperate forest association from 33.55 to 33.06 Ma. This earliest Oligocene recovery in Tasmanian terrestrial temperatures following prior cooling across the EOT coincides with a rebound of atmospheric pCO$_2$ at the earliest Oligocene glacial maximum (EOGM; Pearson et al., 2009) coupled with ice sheet expansion in Antarctica (Galeotti et al., 2016) and sustained deepening of the Tasmanian Gateway (Stickley et al., 2004).

Our study shows that, against a backdrop of global cooling in the late Eocene (a sustained decline in pCO$_2$), a series of regional events in the marine realm, including a change in the stratification of water masses, sequestration of carbon from surface water, and changes in the ocean circulation due to Tasmanian-Gateway-accelerated deepening, may have had a knock-on effect in driving terrestrial climate and vegetation change in the Tasmanian Gateway region.

Data availability. All data are available for download from the Zenodo data repository at https://doi.org/10.5281/zenodo.5924930 (Amoo et al., 2021).

Author contributions. MA and US conceived, designed, and led this study. PKB supplied the palynological samples for this study and provided the biomarker thermometry data. MA and US undertook palynological analyses. MA interpreted palynological data and performed sporomorph-based bioclimatic analyses. MJP and NT provided guidance and expertise with pollen-based palaeoenvironmental reconstruction. MA prepared the manuscript with contributions from US, PKB, MJP, and NT.

Competing interests. The contact author has declared that neither they nor their co-authors have any competing interests.

Disclaimer. Publisher's note: Copernicus Publications remains neutral with regard to jurisdictional claims in published maps and institutional affiliations.

Acknowledgements. Samples for this study were supplied by the Ocean Drilling Program (ODP) sponsored by the US National Science Foundation under the management of the Joint Oceanographic Institutions (JOI). Florian Schwarz is thanked for providing technical support regarding sporomorph-based climate estimate calculations. The authors thank Ian Sluiter and an anonymous reviewer for their helpful comments that have greatly improved our manuscript.

Nick Thompson received funding from the Natural Environment Research Council (NERC)-funded Doctoral Training Partnership ONE Planet [NE/S007512/1]. Peter K. Bijl acknowledges funding from the European Research Council for starting grant number 802835, OceaNice.

Financial support. This research has been supported by the Northumbria University Research Development Fund (RDF), the Natural Environment Research Council (grant no. NE/S007512/1) and the European Research Council, H2020 European Research Council (OceaNice (grant no. 802835)).

Review statement. This paper was edited by Alberto Reyes and reviewed by one anonymous referee.

References

Amoo, M., Salzmann, U., Pound, J. M., Thompson, N., and Bijl, K. P.: Eocene to Oligocene vegetation and climate in the Tasmanian Gateway region controlled by changes in ocean currents and pCO_2, Zenodo [data set], https://doi.org/10.5281/zenodo.5924930, 2021.

Anagnostou, E., John, E. H., Edgar, K. M., Foster, G. L., Ridgwell, A., Inglis, G. N., Pancost, R. D., Lunt, D. J., and Pearson, P. N.: Changing atmospheric CO_2 concentration was the primary driver of early Cenozoic climate, Nature, 533, 380–384, https://doi.org/10.1038/nature17423, 2016.

Askin, R. A.: Spores and pollen from the McMurdo Sound Erratics, Antarctica, in: Paleobiology and Paleoenvironments of Eocene Rocks, McMurdo Sound, East Antarctica, vol. 76, edited by: Stillwell, J. D. and Feldmann, R. M., American Geophysical Union Antarctic Research Series, 161–181, ISBN 9781118668221, 2000.

Askin, R. A. and Raine, J. I.: Oligocene and Early Miocene Terrestrial Palynology of the Cape Roberts Drillhole CRP-2/2A, Victoria Land Basin, Antarctica, Terra Antarct., 7, 493–501, 2000.

Baatsen, M., van Hinsbergen, D. J. J., von der Heydt, A. S., Dijkstra, H. A., Sluijs, A., Abels, H. A., and Bijl, P. K.: Reconstructing geographical boundary conditions for palaeoclimate modelling during the Cenozoic, Clim. Past, 12, 1635–1644, https://doi.org/10.5194/cp-12-1635-2016, 2016.

Benbow, M. C., Alley, N. F., Callan, R. A., and Greenwood, D. R.: Geological history and palaeoclimate, edited by: Dexel, J. F. and Preiss, W. V., Adelaide, 208–217, ISBN 978-0-730-84147-0, 1995.

Biffin, E., Brodribb, T. J., Hill, R. S., Thomas, P., and Lowe, A. J.: Leaf evolution in Southern Hemisphere conifers tracks the angiosperm ecological radiation, Proc. R. Soc. B Biol. Sci., 279, 341–348, https://doi.org/10.1098/rspb.2011.0559, 2012.

Bijl, P. K., Bendle, J. A. P., Bohaty, S. M., Pross, J., Schouten, S., Tauxe, L., Stickley, C. E., McKay, R. M., Röhl, U., Olney, M., Sluijs, A., Escutia, C., Brinkhuis, H., Klaus, A., Fehr, A., Williams, T., Carr, S. A., Dunbar, R. B., Gonzàlez, J. J., Hayden, T. G., Iwai, M., Jimenez-Espejo, F. J., Katsuki, K., Kong, G. S., Nakai, M., Passchier, S., Pekar, S. F., Riesselman, C., Sakai, T., Shrivastava, P. K., Sugisaki, S., Tuo, S., van de Flierdt, T., Welsh, K., and Yamane, M.: Eocene cooling linked to early flow across the Tasmanian Gateway, P. Natl. Acad. Sci. USA, 110, 9645–9650, https://doi.org/10.1073/pnas.1220872110, 2013.

Bijl, P. K., Frieling, J., Cramwinckel, M. J., Boschman, C., Sluijs, A., and Peterse, F.: Maastrichtian–Rupelian paleoclimates in the southwest Pacific – a critical re-evaluation of biomarker paleothermometry and dinoflagellate cyst paleoecology at Ocean Drilling Program Site 1172, Clim. Past, 17, 2393–2425, https://doi.org/10.5194/cp-17-2393-2021, 2021.

Birks, H. J. B. and Line, J. M.: The use of rarefaction analysis for estimating palynological richness from Quaternary pollen-analytical data, Holocene, 2, 1–10, https://doi.org/10.1177/095968369200200101, 1992.

Birks, H. J. B., Felde, V. A., Bjune, A. E., Grytnes, J. A., Seppä, H., and Giesecke, T.: Does pollen-assemblage richness reflect floristic richness? A review of recent developments and future challenges, Rev. Palaeobot. Palynol., 228, 1–25, https://doi.org/10.1016/j.revpalbo.2015.12.011, 2016.

Boland, D., Brooker, M., Chippendale, G., Hall, N., Hyland, B., Johnston, R., Kleinig, D., McDonald, M., and Turner, J.: Forest trees of Australia, 5th edn., CSIRO, Melbourne, ISBN 978-0643069695, 2006.

Bowman, V. C., Francis, J. E., Askin, R. A., Riding, J. B., and Swindles, G. T.: Latest Cretaceous-earliest Paleogene vegetation and climate change at the high southern latitudes: Palynological evidence from Seymour Island, Antarctic Peninsula, Palaeogeogr. Palaeoclimatol. Palaeoecol., 408, 26–47, https://doi.org/10.1016/j.palaeo.2014.04.018, 2014.

Cande, S. C. and Stock, J. M.: Cenozoic reconstruction of the Australia-New Zealand-south Pacific sector of Antarctica, in: The Cenozoic Southern Ocean: Tectonics, sedimentation and climate change between Australia and Antarctica, edited by: Exon, N. F., Kennett, J. P., and Malone, M. J., Geophysical Monograph Series, American Geophysical Union, 5–18, https://doi.org/10.1029/151GM02, 2004.

Cantrill, D. J. and Poole, I.: After the heat: late Eocene to Pliocene climatic cooling and modification of the Antarctic vegetation, in: The Vegetation of Antarctica through Geological Time, edited by: Cantrill, D. J. and Poole, I., Cambridge University Press, Cambridge, ISBN 9780521855983, 2012.

Carpenter, R. J., Jordan, G. J., Mildenhall, D. C., and Lee, D. E.: Leaf fossils of the ancient Tasmanian relict Microcachrys (Podocarpaceae) from New Zealand, Am. J. Bot., 98, 1164–1172, https://doi.org/10.3732/ajb.1000506, 2011.

Carpenter, R. J., Jordan, G. J., Macphail, M. K., and Hill, R. S.: Near-tropical Early Eocene terrestrial temperatures at the Australo-Antarctic margin, western Tasmania, Geology, 40, 267–270, https://doi.org/10.1130/G32584.1, 2012.

Cavalli-Sforza, L. L. and Edwards, A. W.: Phylogenetic analysis, Am. J. Hum. Genet., 19, 233–257, 1967.

Christophel, D. C. and Greenwood, D. R.: Changes in climate and vegetation in Australia during the tertiary, Rev. Palaeobot. Palynol., 58, 97–109, https://doi.org/10.1016/0034-6667(89)90079-1, 1989.

Christophel, D. C., Harris, W. K., and Syber, A. K.: The Eocene flora of the Anglesea Locality, Victoria, Alcheringa, 11, 303–323, https://doi.org/10.1080/03115518708619139, 1987.

Colwyn, D. A. and Hren, M. T.: An abrupt decrease in Southern Hemisphere terrestrial temperature during the Eocene–Oligocene transition, Earth Planet. Sci. Lett., 512, 227–235, https://doi.org/10.1016/j.epsl.2019.01.052, 2019.

Contreras, L., Pross, J., Bijl, P. K., Koutsodendris, A., Raine, J. I., van de Schootbrugge, B., and Brinkhuis, H.: Early to Middle Eocene vegetation dynamics at the Wilkes Land Margin (Antarctica), Rev. Palaeobot. Palynol., 197, 119–142, https://doi.org/10.1016/j.revpalbo.2013.05.009, 2013.

Contreras, L., Pross, J., Bijl, P. K., O'Hara, R. B., Raine, J. I., Sluijs, A., and Brinkhuis, H.: Southern high-latitude terrestrial climate change during the Palaeocene–Eocene derived from a marine pollen record (ODP Site 1172, East Tasman Plateau), Clim. Past, 10, 1401–1420, https://doi.org/10.5194/cp-10-1401-2014, 2014.

Cooper, W. and Cooper, W.: Fruits of the Australian tropical rainforest, Nokomis Publications, Clifton Hill, Victoria, ISBN 978-0-958-17421-3, 2004.

Coxall K., H., Wilson A., P., Palike, H., Lear H., C., and Backman, J.: Rapid stepwise onset of Antarctic glaciation and deeper calcite compensation in the Pacific Ocean, Nature, 433, 53–57, https://doi.org/10.1038/nature03135, 2005.

Daly, R. J., Jolley, D. W., Spicer, R. A., and Ahlberg, A.: A palynological study of an extinct arctic ecosystem from the Palaeocene of Northern Alaska, Rev. Palaeobot. Palynol., 166, 107–116, https://doi.org/10.1016/j.revpalbo.2011.05.008, 2011.

DeConto, R. M. and Pollard, D.: Rapid Cenozoic glaciation of Antarctica induced by declining atmospheric CO_2, Nature, 1317, 245–249, https://doi.org/10.1038/nature01290, 2003.

Dettmann, M. E., Pocknall, D. T., Romero, E. J., and Zamaloa, M. del C.: Nothofagidites Erdtman ex Potonie, 1960; a catalogue of species with notes on the paleogeographic distribution of Nothofagus Bl. (southern beech), New Zeal. Geol. Surv. Paleontol. Bull., 60, 1–77, 1990.

De Vleeschouwer, D., Vahlenkamp, M., Crucifix, M., and Pälike, H.: Alternating Southern and Northern Hemisphere climate response to astronomical forcing during the past 35 m.y., Geology, 45, 375–378, https://doi.org/10.1130/G38663.1, 2017.

Dowe, J. L.: Australian Palms, CSIRO Publishing, Victoria, ISBN 978-0-643-09802-2, 2010.

Emanuel, W. R., Shugart, H. H., and Stevenson, M. P.: Climatic change and the broad-scale distribution of terrestrial ecosystem complexes, Clim. Change, 7, 29–43, https://doi.org/10.1007/BF00139439, 1985.

Evi, E., Hill, R. S., and Scriven, L. J.: The angiosperm-dominated woody vegetation of Antarctica: a review, Rev. Palaeobot. Palynol., 86, 175–198, 1995.

Exon, N. F., Berry, R. F., Crawford, A. J., and Hill, P. J.: Geological evolution of the East Tasman Plateau, a continental fragment southeast of Tasmania, Aust. J. Earth Sci., 44, 597–608, https://doi.org/10.1080/08120099708728339, 1997.

Exon, N. F., Kennett, J. P., and Malone, M. J.: Proceedings of the Ocean Drilling Program, 189 Initial Reports, Ocean Drilling Program, https://doi.org/10.2973/odp.proc.ir.189.2001, 2001.

Exon, N. F., Kennett, J. P., and Malone, M. J.: Leg 189 synthesis: Cretaceous-Holocene history of the Tasmanian gateway, Proc. Ocean Drill. Progr. Sci. Results, Ocean Drilling Program, https://doi.org/10.2973/odp.proc.sr.189.101.2004, 2004a.

Exon, N. F., Kennett, J. P., and Malone, M. J.: The Cenozoic Southern Ocean: Tectonics, sedimentation and climate change between Australia and Antarctica, Geophysical Monograph Series, 151, American Geophysical Union, Washington, ISBN 978-0-875-90416-0, 2004b.

Farjon, A.: A handbook of the World's Conifers, Koninklijke Brill, Leiden, the Netherlands, ISBN 9789047430629, 2010.

Fick, S. E. and Hijmans, R. J.: WorldClim 2: new 1-km spatial resolution climate surfaces for global land areas, Int. J. Climatol., 37, 4302–4315, https://doi.org/10.1002/joc.5086, 2017.

Francis, J. E., Marenssi, S., Levy, R., Hambrey, M., Thorn, V. C., Mohr, B., Brinkhuis, H., Warnaar, J., Zachos, J., Bohaty, S., and DeConto, R.: From Greenhouse to Icehouse – The Eocene/Oligocene in Antarctica, Dev. Earth Environ. Sci., 8, 309–368, https://doi.org/10.1016/S1571-9197(08)00008-6, 2008.

Fuller, M. and Touchard, Y.: On the magnetostratigraphy of the East Tasman Plateau, timing of the opening of the Tasmanian Gateway and paleoenvironmental changes, in: The Cenozoic Southern Ocean: tectonics, sedimentation and climate change between Australia and Antarctica, edited by: Exon, N., Kennett, J. P., and Malone, M., American Geophysical Union, Geophysical Monograph series, Washington, 127–151, ISBN 978-0-875-90416-0, 2004.

Gaina, C., Müller, R. D., Royer, J.-Y., and Symonds, P.: Evolution of the Louisiade triple junction, J. Geophys. Res.-Sol. Ea., 104, 12927–12939, https://doi.org/10.1029/1999JB900038, 1999.

Galeotti, S., DeConto, R., Naish, T., Stocchi, P., Florindo, F., Pagani, M., Barrett, P., Bohaty, S. M., Lanci, L., Pollard, D., Sandroni, S., Talarico, F. M., and Zachos, J. C.: Antarctic Ice Sheet variability across the Eocene-Oligocene boundary climate transition, Science, 352, 76–80, https://doi.org/10.1126/science.aab0669, 2016.

GBIF: GBIF Occurrence Download, Global Biodiversity Information Facility [data set], https://doi.org/10.15468/dl.nckq6t, 2021.

Goldner, A., Herold, N., and Huber, M.: Antarctic glaciation caused ocean circulation changes at the Eocene-Oligocene transition, Nature, 511, 574–577, https://doi.org/10.1038/nature13597, 2014.

Grimm, E. C.: CONISS: a FORTRAN 77 program for stratigraphically constrained cluster analysis by the method of incremental sum of squares, Comput. Geosci., 13, 13–35, https://doi.org/10.1016/0098-3004(87)90022-7, 1987.

Grimm, E. C.: Tilia and Tiliagraph, PC spreadsheet and graphics software for pollen data, INQUA Work. Gr. Data Handl. Methods, Newsl., 4, 5–7, 1990.

Hammer, Ø., Harper, D. A. T., and Ryan, P. D.: Past: Paleontological statistics software package for education and data analysis, Palaeontol. Electron., 4, 178, 2001.

Harbert, R. S. and Nixon, K. C.: Climate reconstruction analysis using coexistence likelihood estimation (CRACLE): A method for the estimation of climate using vegetation, Am. J. Bot., 102, 1277–1289, https://doi.org/10.3732/ajb.1400500, 2015.

Hayek, L. C. and Buzas, M. A.: Surveying Natural Populations, Columbia University Press, New York, ISBN 9780231146203, 2010.

Heureux, A. M. C. and Rickaby, R. E. M.: Refining our estimate of atmospheric CO_2 across the Eocene-Oligocene climatic transition, Earth Planet. Sci. Lett., 409, 329–338, https://doi.org/10.1016/j.epsl.2014.10.036, 2015.

Hijmans, R. J., Phillips, S., Leathwick, J., and Elith, J.: dismo: Species distribution modelling, R Packag. version, 1(4), 1, https://cran.r-project.org/web/packages/dismo/index.html (last access: 28 September 2021), 2017.

Hill, M. O. and Gauch, H. G.: Detrended correspondence analysis: An improved ordination technique, Vegetatio, 43, 47–58, 1980.

Hill, P. J. and Exon, N. F.: Tectonics and basin development of the offshore Tasmanian area; incorporating results from deep ocean drilling, in: The Cenozoic Southern Ocean; tectonics, sedimen-

tation and climate between Australia and Antarctica, edited by: Exon, N. F., Kennett, J. P., and Malone, M., Geophysical Monograph Series, 151, American Geophysical Union, Washington, 19–19, ISBN 978-0-875-90416-0, 2004.

Hill, R. S. (Ed.): History of the Australian Vegetation: Cretaceous to Recent, University of Adelaide Press, https://doi.org/10.20851/australian-vegetation, 1994.

Hill, R. S. (Ed.): History of the Australian Vegetation: Cretaceous to Recent, University of Adelaide Press, ISBN 978-1-925261-47-9, 2017.

Hill, R. S. and Dettmann, E. M.: Origin and diversification of the Genus Nothofagus, in: The Ecology and Biogeography of Nothofagus forests, edited by: Veblen, T. T., Hill, S. R., and Read, J., Yale University Press, New Haven, 11–24, ISBN 0-300-06423-3, 1996.

Hill, R. S. and Macphail, M. K.: Reconstruction of the Oligocene vegetation at Pioneer, northeast Tasmania, Alcheringa, 7, 281–299, https://doi.org/10.1080/03115518308619613, 1983.

Hill, R. S., Whang, S. S., Korasidis, V., Bianco, B., Hill, K. E., Paull, R., and Guerin, G. R.: Fossil evidence for the evolution of the Casuarinaceae in response to low soil nutrients and a drying climate in Cenozoic Australia, Aust. J. Bot., 68, 179–194, https://doi.org/10.1071/BT19126, 2020.

Hoem, F. S., Valero, L., Evangelinos, D., Escutia, C., Duncan, B., McKay, R. M., Brinkhuis, H., Sangiorgi, F., and Bijl, P. K.: Temperate Oligocene surface ocean conditions offshore of Cape Adare, Ross Sea, Antarctica, Clim. Past, 17, 1423–1442, https://doi.org/10.5194/cp-17-1423-2021, 2021.

Holdgate, G. R., Sluiter, I. R. K., and Taglieri, J.: Eocene-Oligocene coals of the Gippsland and Australo-Antarctic basins – Paleoclimatic and paleogeographic context and implications for the earliest Cenozoic glaciations, Palaeogeogr. Palaeoclimatol. Palaeoecol., 472, 236–255, https://doi.org/10.1016/j.palaeo.2017.01.035, 2017.

Hollis, C. J., Dunkley Jones, T., Anagnostou, E., Bijl, P. K., Cramwinckel, M. J., Cui, Y., Dickens, G. R., Edgar, K. M., Eley, Y., Evans, D., Foster, G. L., Frieling, J., Inglis, G. N., Kennedy, E. M., Kozdon, R., Lauretano, V., Lear, C. H., Littler, K., Lourens, L., Meckler, A. N., Naafs, B. D. A., Pälike, H., Pancost, R. D., Pearson, P. N., Röhl, U., Royer, D. L., Salzmann, U., Schubert, B. A., Seebeck, H., Sluijs, A., Speijer, R. P., Stassen, P., Tierney, J., Tripati, A., Wade, B., Westerhold, T., Witkowski, C., Zachos, J. C., Zhang, Y. G., Huber, M., and Lunt, D. J.: The DeepMIP contribution to PMIP4: methodologies for selection, compilation and analysis of latest Paleocene and early Eocene climate proxy data, incorporating version 0.1 of the DeepMIP database, Geosci. Model Dev., 12, 3149–3206, https://doi.org/10.5194/gmd-12-3149-2019, 2019.

Homes, A. M., Cieraad, E., Lee, D. E., Lindqvist, J. K., Raine, J. I., Kennedy, E. M., and Conran, J. G.: A diverse fern flora including macrofossils with in situ spores from the late Eocene of southern New Zealand, Rev. Palaeobot. Palynol., 220, 16–28, https://doi.org/10.1016/j.revpalbo.2015.04.007, 2015.

Houben, A. J. P., van Mourik, C. A., Montanari, A., Coccioni, R., and Brinkhuis, H.: The Eocene–Oligocene transition: Changes in sea level, temperature or both?, Palaeogeogr. Palaeoclimatol. Palaeoecol., 335, 335–336, https://doi.org/10.1016/j.palaeo.2011.04.008, 2012.

Houben, A. J. P., Bijl, P. K., Sluijs, A., Schouten, S., and Brinkhuis, H.: Late Eocene Southern Ocean cooling and invigoration of circulation preconditioned Antarctica for full-scale glaciation, Geochem. Geophy. Geosy., 20, 2214–2234, https://doi.org/10.1029/2019GC008182, 2019.

Huber, M., Brinkhuis, H., Stickley, C. E., Döös, K., Sluijs, A., Warnaar, J., Schellenberg, S. A., and Williams, G. L.: Eocene circulation of the Southern Ocean: Was Antarctica kept warm by subtropical waters?, Paleoceanography, 19, 1–12, https://doi.org/10.1029/2004PA001014, 2004.

Hutchinson, D. K., Coxall, H. K., Lunt, D. J., Steinthorsdottir, M., de Boer, A. M., Baatsen, M., von der Heydt, A., Huber, M., Kennedy-Asser, A. T., Kunzmann, L., Ladant, J.-B., Lear, C. H., Moraweck, K., Pearson, P. N., Piga, E., Pound, M. J., Salzmann, U., Scher, H. D., Sijp, W. P., Śliwińska, K. K., Wilson, P. A., and Zhang, Z.: The Eocene–Oligocene transition: a review of marine and terrestrial proxy data, models and model–data comparisons, Clim. Past, 17, 269–315, https://doi.org/10.5194/cp-17-269-2021, 2021.

Huurdeman, E. P., Frieling, J., Reichgelt, T., Bijl, P. K., Bohaty, S. M., Holdgate, G. R., Gallagher, S. J., Peterse, F., Greenwood, D. R., and Pross, J.: Rapid expansion of meso-megathermal rain forests into the southern high latitudes at the onset of the Paleocene-Eocene Thermal Maximum, Geology, 49, 40–44, https://doi.org/10.1130/G47343.1, 2021.

Hyland, B. P. M.: Carnarvonia, in Flora of Australia, Elaeagnaceae, Proteaceae 1, edited by: McCarthy, P., CSIRO Publishing/Australian Biological Resources Study, CANBERRA, vol. 16, 343–345, ISBN 0643056939, 1995.

Katz, M. E., Miller, K. G., Wright, J. D., Wade, B. S., Browning, J. V., Cramer, B. S., and Rosenthal, Y.: Stepwise transition from the Eocene greenhouse to the Oligocene icehouse, Nat. Geosci., 1, 329–334, https://doi.org/10.1038/ngeo179, 2008.

Kemp, E. M.: Tertiary climatic evolution and vegetation history in the Southeast Indian Ocean region, Palaeogeogr. Palaeoclimatol. Palaeoecol., 24, 169–208, https://doi.org/10.1016/0031-0182(78)90042-1, 1978.

Kennett, J. P.: Cenozoic evolution of Antarctic glaciation, the circum-Antarctic Ocean, and their impact on global paleoceanography, J. Geophys. Res., 82, 3843–3860, https://doi.org/10.1029/jc082i027p03843, 1977.

Kershaw, A. P.: Australasia, in: Vegetation History, edited by: Huntley, B. and Webb, T., Kluwer Academic Publishers, Dordrecht, 111, 237–306, ISBN 9061931886, 1988.

Kershaw, P. and Wagstaff, B.: The southern conifer family Araucariaceae: History, status, and value for paleoenvironmental reconstruction, Annu. Rev. Ecol. Syst., 32, 397–414, https://doi.org/10.1146/annurev.ecolsys.32.081501.114059, 2001.

Klages, J. P., Salzmann, U., Bickert, T., Hillenbrand, C. D., Gohl, K., Kuhn, G., Bohaty, S. M., Titschack, J., Müller, J., Frederichs, T., Bauersachs, T., Ehrmann, W., van de Flierdt, T., Pereira, P. S., Larter, R. D., Lohmann, G., Niezgodzki, I., Uenzelmann-Neben, G., Zundel, M., Spiegel, C., Mark, C., Chew, D., Francis, J. E., Nehrke, G., Schwarz, F., Smith, J. A., Freudenthal, T., Esper, O., Pälike, H., Ronge, T. A., Dziadek, R., Afanasyeva, V., Arndt, J. E., Ebermann, B., Gebhardt, C., Hochmuth, K., Küssner, K., Najman, Y., Riefstahl, F., and Scheinert, M.: Temperate rainforests

near the South Pole during peak Cretaceous warmth, Nature, 580, 81–86, https://doi.org/10.1038/s41586-020-2148-5, 2020.

Korasidis, V. A., Wallace, M. W., Wagstaff, B. E., and Hill, R. S.: Terrestrial cooling record through the Eocene-Oligocene transition of Australia, Glob. Planet. Change, 173, 61–72, https://doi.org/10.1016/j.gloplacha.2018.12.007, 2019.

Kühl, N., Gebhardt, C., Litt, T., and Hense, A.: Probability density functions as botanical-climatological transfer functions for climate reconstruction, Quat. Res., 58, 381–392, https://doi.org/10.1006/qres.2002.2380, 2002.

Kumaran, N., Punekar, S., and Limaye, R.: Palaeoclimate and phytogeographical appraisal of Neogene pollen record from India, J. Palynol., 46, 315–330, 2011.

Ladant, J.-B., Donnadieu, Y., and Dumas, C.: Links between CO_2, glaciation and water flow: reconciling the Cenozoic history of the Antarctic Circumpolar Current, Clim. Past, 10, 1957–1966, https://doi.org/10.5194/cp-10-1957-2014, 2014.

Lanyon, R., Varne, R., and Crawford, A. J.: Tasmanian Tertiary basalts, the Balleny plume, and opening of the Tasman Sea (southwest Pacific Ocean), Geology, 21, 555–558, https://doi.org/10.1130/0091-7613(1993)021<0555:TTBTBP>2.3.CO;2, 1993.

Lauretano, V., Kennedy-Asser, A. T., Korasidis, V. A., Wallace, M. W., Valdes, P. J., Lunt, D. J., Pancost, R. D., and Naafs, B. D. A.: Eocene to Oligocene terrestrial Southern Hemisphere cooling caused by declining pCO_2, Nat. Geosci., 14, 659–664, https://doi.org/10.1038/s41561-021-00788-z, 2021.

Lear, C. H., Bailey, T. R., Pearson, P. N., Coxall, H. K., and Rosenthal, Y.: Cooling and ice growth across the Eocene-Oligocene transition, Geology, 36, 251–254, https://doi.org/10.1130/G24584A.1, 2008.

Lee, D. E., Lee, W. G., Jordan, G. J., and Barreda, V. D.: The Cenozoic history of New Zealand temperate rainforests: comparisons with southern Australia and South America, New Zeal. J. Bot., 54, 100–127, https://doi.org/10.1080/0028825X.2016.1144623, 2016.

Legendre, P. and Legendre, F.: Numerical Ecology, 3rd edn., Elsevier, ISBN 9780444538697, 2012.

Liu, Z., Pagani, M., Zinniker, D., DeConto, R., Huber, M., Brinkhuis, H., Shah, S. R., Leckie, R. M., and Pearson, A.: Global cooling during the Eocene-Oligocene climate transition, Science, 323, 1187–1190, https://doi.org/10.1126/science.1166368, 2009.

López-Quirós, A., Escutia, C., Etourneau, J., Rodríguez-Tovar, F. J., Roignant, S., Lobo, F. J., Thompson, N., Bijl, P. K., Bohoyo, F., Salzmann, U., Evangelinos, D., Salabarnada, A., Hoem, F. S., and Sicre, M. A.: Eocene-Oligocene paleoenvironmental changes in the South Orkney Microcontinent (Antarctica) linked to the opening of Powell Basin, Glob. Planet. Change, 204, 103581, https://doi.org/10.1016/j.gloplacha.2021.103581, 2021.

Mabberley, D. J.: The Plant-Book, 2nd edn., Cambridge University Press, ISBN 9780521414210, 1997.

Macphail, M. and Cantrill, D. J.: Age and implications of the Forest Bed, Falkland Islands, southwest Atlantic Ocean: Evidence from fossil pollen and spores, Palaeogeogr. Palaeoclimatol. Palaeoecol., 240, 602–629, https://doi.org/10.1016/j.palaeo.2006.03.010, 2006.

Macphail, M., Alley, F., Truswell, E., and Sluiter, I. R. K.: Early Tertiary vegetation: Evidence from spores and pollen, in: History of the Australian Vegetation: Cretaceous to Recent, edited by: Hill, R. S., Cambridge University Press, Cambridge, 189–261, https://doi.org/10.20851/australian-vegetation, 1994.

Macphail, M. K.: Palynostratigraphy of the murray basin, inland Southeastern Australia, Palynology, 23, 197–240, https://doi.org/10.1080/01916122.1999.9989528, 1999.

Macphail, M. K.: Australian Palaeoclimates: Cretaceous to Tertiary – A review of palaeobotanical and related evidence to the year 2000, CRC LEME Spec. Vol. Open File Rep. 151, 266 pp., ISBN 1921039752, 2007.

Macphail, M. K. and Hill, R. S.: What was the vegetation in northwest Australia during the Paleogene, 66–23 million years ago?, Aust. J. Bot., 66, 556–574, https://doi.org/10.1071/BT18143, 2018.

Macphail, M. K. and Truswell, E. M.: Palynology of Site 1166, Prydz Bay, East Antarctica, in: Proceedings of the Ocean Drilling Program, Scientific Results, edited by: Cooper, A. K., O'Brien, P. E., and Richter, C., Ocean Drilling Program, vol. 188, 1–43, https://doi.org/10.2973/odp.proc.sr.188.2004, 2004.

Macphail, M. K., Pemberton, M., and Jacobson, G.: Peat mounds of southwest Tasmania: Possible origins, Aust. J. Earth Sci., 46, 667–677, https://doi.org/10.1046/j.1440-0952.1999.00736.x, 1999.

Martin, H.: Australian Tertiary phytogeography: Evidence for palynology, in: History of the Australian vegetation: Cretaceous to Holocene, edited by: Hill, R. S., Cambridge University Press, Cambridge, 104–142, https://doi.org/10.20851/australian-vegetation, 1994.

Martin, H. A.: Cenozoic climatic change and the development of the arid vegetation in Australia, J. Arid Environ., 66, 533–563, https://doi.org/10.1016/j.jaridenv.2006.01.009, 2006.

Mosbrugger, V.: The nearest living relative method, in: Fossil Plants and Spores: Modern Techniques, edited by: Jones, T. P. and Rowe, N. P., Geological Society, London, 261–265, ISBN 978-1-86239-035-5, 1999.

Mosbrugger, V. and Utescher, T.: The coexistence approach – A method for quantitative reconstructions of Tertiary terrestrial palaeoclimate data using plant fossils, Palaeogeogr. Palaeoclimatol. Palaeoecol., 134, 61–86, https://doi.org/10.1016/S0031-0182(96)00154-X, 1997.

Myerscough, P., Whelan, R., and Bradstock, R.: Ecology of Proteaceae with special reference to the Sydney region, Cunninghamia, 6, 951–1015, 2007.

Naafs, B. D. A., Inglis, G. N., Zheng, Y., Amesbury, M. J., Biester, H., Bindler, R., Blewett, J., Burrows, M. A., del Castillo Torres, D., Chambers, F. M., Cohen, A. D., Evershed, R. P., Feakins, S. J., Gałka, M., Gallego-Sala, A., Gandois, L., Gray, D. M., Hatcher, P. G., Honorio Coronado, E. N., Hughes, P. D. M., Huguet, A., Könönen, M., Laggoun-Défarge, F., Lähteenoja, O., Lamentowicz, M., Marchant, R., McClymont, E., Pontevedra-Pombal, X., Ponton, C., Pourmand, A., Rizzuti, A. M., Rochefort, L., Schellekens, J., De Vleeschouwer, F., and Pancost, R. D.: Introducing global peat-specific temperature and pH calibrations based on brGDGT bacterial lipids, Geochim. Cosmochim. Ac., 208, 285–301, https://doi.org/10.1016/j.gca.2017.01.038, 2017.

Ogden, J., Stewart, G. H., and Allen, R. B.: Ecology of New Zealand Nothofagus Forest, in: The Ecology and Biogeography of Nothofagus Forests, edited by: Veblen, T. T., Hill, R. S., and

Read, J., Yale University Press, New Haven and London, 25–82, ISBN 0-300-06423-3, 1996.

Oksanen, J., Blanchet, F. G., Friendly, M., Kindt, R., Legendre, P., McGlinn, D., Minchin, P. R., O'Hara, R. B., Simpson, G. L., Solymos, P., Stevens, M. H. H., Szoecs, E., and Wagner, H.: Vegan: community ecology package, R Packag. version 2.5-6, https://cran.r-project.org/package=vegan (last access: 9 August 2021), 2019.

Pagani, M., Huber, M., Liu, Z., Bohaty, S. M., Henderiks, J., Sijp, W., Krishnan, S., and DeConto, R. M.: The role of Carbon dioxide during the onset of Antarctic glaciation, Science, 334, 1261–1264, https://doi.org/10.1126/science.1203909, 2011.

Pälike, H., Norris, R. D., Herrle, J. O., Wilson, P. A., Coxall, H. K., Lear, C. H., Shackleton, N. J., Tripati, A. K., and Wade, B. S.: The heartbeat of the Oligocene climate system, Science, 314, 1894–1898, https://doi.org/10.1126/science.1133822, 2006.

Partridge, A. and Dettmann, M.: Plant microfossils, in: Geology of Victoria, edited by: Birch, W. D., Geological Society of Australia Special Publication, 639–652, ISBN 18761253301, 2003.

Partridge, D. A.: New observations on the Cenozoic stratigraphy of the Bassian Rise derived from a palynological study of the Groper-1, Mullet-1 and Bluebone-1 wells, offshore Gippsland Basin, southeast Australia, https://www.mrt.tas.gov.au/mrtdoc/petxplor/download/OR_0675/BR2006_07.pdf (last access: 1 January 2022), 2006.

Passchier, S., Ciarletta, D. J., Miriagos, T. E., Bijl, P. K., and Bohaty, S. M.: An Antarctic stratigraphic record of stepwise ice growth through the Eocene-Oligocene transition, Bull. Geol. Soc. Am., 129, 318–330, https://doi.org/10.1130/B31482.1, 2017.

Pearson, P. N., Foster, G. L., and Wade, B. S.: Atmospheric carbon dioxide through the Eocene–Oligocene climate transition, Nature, 461, 1110–1113, https://doi.org/10.1038/nature08447, 2009.

Pocknall, D. T.: Palynology of Waikato Coal Measures (Late Eocene-late Oligocene) from the Raglan area, North Island, New Zealand, New Zeal. J. Geol. Geophys., 28, 329–349, https://doi.org/10.1080/00288306.1985.10422231, 1985.

Pocknall, D. T.: Late Eocene to early Miocene vegetation and climate history of New Zealand, J. R. Soc. New Zeal., 19, 1–18, https://doi.org/10.1080/03036758.1989.10426451, 1989.

Pole, M. S. and Macphail, M. K.: Eocene Nypa from Regatta Point, Tasmania, Rev. Palaeobot. Palynol., 92, 55–67, 1996.

Poole, I., Cantrill, D., and Utescher, T.: A multi-proxy approach to determine Antarctic terrestrial palaeoclimate during the Late Cretaceous and Early Tertiary, Palaeogeogr. Palaeoclimatol. Palaeoecol., 222, 95–121, https://doi.org/10.1016/j.palaeo.2005.03.011, 2005.

Pound, M. J. and Salzmann, U.: Heterogeneity in global vegetation and terrestrial climate change during the late Eocene to early Oligocene transition, Sci. Rep., 7, 43386, https://doi.org/10.1038/srep43386, 2017.

Prebble, J. G., Raine, J. I., Barrett, P. J., and Hannah, M. J.: Vegetation and climate from two Oligocene glacioeustatic sedimentary cycles (31 and 24 Ma) cored by the Cape Roberts Project, Victoria Land Basin, Antarctica, Palaeogeogr. Palaeoclimatol. Palaeoecol., 231, 41–57, https://doi.org/10.1016/j.palaeo.2005.07.025, 2006.

Prebble, J. G., Kennedy, E. M., Reichgelt, T., Clowes, C., Womack, T., Mildenhall, D. C., Raine, J. I., and Crouch, E. M.: A 100 million year composite pollen record from New Zealand shows maximum angiosperm abundance delayed until Eocene, Palaeogeogr. Palaeoclimatol. Palaeoecol., 566, 110207, https://doi.org/10.1016/j.palaeo.2020.110207, 2021.

Pross, J.: Paleo-oxygenation in Tertiary epeiric seas: evidence from dinoflagellate cysts, Palaeogeogr. Palaeoclimatol. Palaeoecol., 166, 369–381, https://doi.org/10.1016/S0031-0182(00)00219-4, 2001.

Pross, J., Klotz, S., and Mosbrugger, V.: Reconstructing palaeotemperatures for the Early and Middle Pleistocene using the mutual climatic range method based on plant fossils, Quat. Sci. Rev., 19, 1785–1799, https://doi.org/10.1016/S0277-3791(00)00089-5, 2000.

Pross, J., Contreras, L., Bijl, P. K., Greenwood, D. R., Bohaty, S. M., Schouten, S., Bendle, J. A., Röhl, U., Tauxe, L., Raine, J. I., Huck, C. E., van de Flierdt, T., Jamieson, S. S. R., Stickley, C. E., van de Schootbrugge, B., Escutia, C., Brinkhuis, H., Brinkhuis, H., Escutia Dotti, C., Klaus, A., Fehr, A., Williams, T., Bendle, J. A. P., Bijl, P. K., Bohaty, S. M., Carr, S. A., Dunbar, R. B., Gonzàlez, J. J., Hayden, T. G., Iwai, M., Jimenez-Espejo, F. J., Katsuki, K., Soo Kong, G., McKay, R. M., Nakai, M., Olney, M. P., Passchier, S., Pekar, S. F., Pross, J., Riesselman, C. R., Röhl, U., Sakai, T., Shrivastava, P. K., Stickley, C. E., Sugisaki, S., Tauxe, L., Tuo, S., van de Flierdt, T., Welsh, K., Yamane, M., and Integrated Ocean Drilling Program Expedition 318 Scientists: Persistent near-tropical warmth on the Antarctic continent during the early Eocene epoch, Nature, 488, 73–77, https://doi.org/10.1038/nature11300, 2012.

Quilty, P. G.: Late Eocene foraminifers and palaeoenvironment, Cascade Seamount, southwest Pacific Ocean: Implications for seamount subsidence and Australia Antarctica Eocene correlation, Aust. J. Earth Sci., 48, 633–641, https://doi.org/10.1046/j.1440-0952.2001.485886.x, 2001.

Raine, J. I., Mildenhall, D. C., and Kennedy, E.: New Zealand fossil spores and pollen: an illustrated catalogue, GNS Science, New Zealand, https://www.gns.cri.nz/what/earthhist/fossils/spore_pollen/catalog/index.htm (last access: 25 December 2021), 2011.

R Core Team: R: A language and environment for statistical computing, R Found. Stat. Comput., https://www.r-project.org/ (last access: 9 August 2021), 2019.

Read, J. and Hill, R. S.: Dynamics of Nothofagus-dominated rainforest on mainland Australia and lowland Tasmania, Vegetatio, 63, 67–78, https://doi.org/10.1007/BF00032607, 1985.

Read, J., Hope, G. S., and Hill, R. S.: Phytogeography and climate analysis of Nothofagus subgenus Brassospora in New Guinea and New Caledonia, Aust. J. Bot., 53, 297–312, https://doi.org/10.1071/BT04155, 2005.

Reichgelt, T., West, C. K., and Greenwood, D. R.: The relation between global palm distribution and climate, Sci. Rep., 8, 2–12, https://doi.org/10.1038/s41598-018-23147-2, 2018.

Royer, J. and Rollet, N.: Plate-tectonic setting of the Tasmanian region, Aust. J. Earth Sci., 44, 543–560, https://doi.org/10.1080/08120099708728336, 1997.

Sanguinetti, J. and Kitzberger, T.: Patterns and mechanisms of masting in the large-seeded southern hemisphere conifer Araucaria araucana, Austral. Ecol., 33, 78–87, https://doi.org/10.1111/j.1442-9993.2007.01792.x, 2008.

Scher, H. D., Bohaty, S. M., Smith, B. W., and Munn, G. H.: Isotopic interrogation of a suspected late Eocene glaciation, Paleoceanography, 29, 628–644, https://doi.org/10.1002/2014PA002648, 2014.

Shannon, C. E.: A Mathematical Theory of Communication, Bell Syst. Tech. J., 27, 379–423, https://doi.org/10.1002/j.1538-7305.1948.tb01338.x, 1948.

Shipboard Scientific Party: Site 1172, in: Proceedings of the Ocean Drilling Program, 189 Initial Reports, edited by: Exon, N. F., Kennett, J. P., and Malone, M. J., Ocean Drilling Program, 1–149, https://doi.org/10.2973/odp.proc.ir.189.107.2001, 2001.

Sijp, W. P., England, M. H., and Huber, M.: Effect of the deepening of the Tasman Gateway on the global ocean, Paleoceanography, 26, 1–18, https://doi.org/10.1029/2011PA002143, 2011.

Stickley, C. E., Brinkhuis, H., Schellenberg, S. A., Sluijs, A., Röhl, U., Fuller, M., Grauert, M., Huber, M., Warnaar, J., and Williams, G. L.: Timing and nature of the deepening of the Tasmanian Gateway, Paleoceanography, 19, 1–18, https://doi.org/10.1029/2004PA001022, 2004.

Thompson, N., Salzmann, U., López-Quirós, A., Bijl, P. K., Hoem, F. S., Etourneau, J., Sicre, M.-A., Roignant, S., Hocking, E., Amoo, M., and Escutia, C.: Vegetation change across the Drake Passage region linked to late Eocene cooling and glacial disturbance after the Eocene–Oligocene transition, Clim. Past, 18, 209–232, https://doi.org/10.5194/cp-18-209-2022, 2022.

Tibbett, E. J., Scher, H. D., Warny, S., Tierney, J. E., Passchier, S., and Feakins, S. J.: Late Eocene record of hydrology and temperature from Prydz Bay, East Antarctica, Paleoceanogr. Paleoclimatol., 36, e2020PA004204, https://doi.org/10.1029/2020PA004204, 2021.

Tripathi, S. K. and Srivastava, D.: Palynology and palynofacies of the early Palaeogene lignite bearing succession of Vastan, Cambay Basin, Western India, Acta Palaeobot., 52, 157–175, 2012.

Truswell, E. M.: Vegetation changes in the Australian tertiary in response to climatic and phytogeographic forcing factors, Aust. Syst. Bot., 6, 533–557, https://doi.org/10.1071/SB9930533, 1993.

Truswell, E. M. and Macphail, M. K.: Polar forests on the edge of extinction: What does the fossil spore and pollen evidence from East Antarctica say?, Aust. Syst. Bot., 22, 57–106, https://doi.org/10.1071/SB08046, 2009.

Utescher, T., Mosbrugger, V., and Ashraf, A. R.: Terrestrial climate evolution in Northwest Germany over the last 25 million years, Palaios, 15, 430–449, https://doi.org/10.2307/3515514, 2000.

Utescher, T., Bruch, A. A., Erdei, B., François, L., Ivanov, D., Jacques, F. M. B., Kern, A. K., Liu, Y. S. C., Mosbrugger, V., and Spicer, R. A.: The Coexistence Approach-Theoretical background and practical considerations of using plant fossils for climate quantification, Palaeogeogr. Palaeoclimatol. Palaeoecol., 410, 58–73, https://doi.org/10.1016/j.palaeo.2014.05.031, 2014.

Vajda, V., Raine, J. I., and Hollis, C. J.: Indication of global deforestation at the Cretaceous-Tertiary boundary by New Zealand fern spike, Science, 294, 1700–1702, https://doi.org/10.1126/science.1064706, 2001.

Veblen, T. T.: Regeneration Patterns in Araucaria araucana Forests in Chile, J. Biogeogr., 9, 11–28, https://doi.org/10.2307/2844727, 1982.

Veblen, T. T., Hill, R. S., and Read, J.: The ecology and biogeography of Nothofagus forests, Yale University Press, New Haven, ISBN 0-300-6423-3, 1996.

Verma, P., Garg, R., Rao, M. R., and Bajpai, S.: Palynofloral diversity and palaeoenvironments of early Eocene Akri lignite succession, Kutch Basin, western India, Palaeobio. Palaeoenv., 100, 605–627, https://doi.org/10.1007/s12549-019-00388-1, 2020.

Villa, G., Fioroni, C., Pea, L., Bohaty, S., and Persico, D.: Middle Eocene-late Oligocene climate variability: Calcareous nannofossil response at Kerguelen Plateau, Site 748, Mar. Micropaleontol., 69, 173–192, https://doi.org/10.1016/j.marmicro.2008.07.006, 2008.

Villa, G., Fioroni, C., Persico, D., Roberts, A. P., and Florindo, F.: Middle Eocene to Late Oligocene Antarctic glaciation/deglaciation and Southern Ocean productivity, Paleoceanography, 29, 223–237, https://doi.org/10.1002/2013PA002518, 2014.

Willard, D. A., Donders, T. H., Reichgelt, T., Greenwood, D. R., Sangiorgi, F., Peterse, F., Nierop, K. G. J., Frieling, J., and Schouten, S.: Arctic vegetation, temperature, and hydrology during Early Eocene transient global warming events, Glob. Planet. Change, 178, 139–152, https://doi.org/10.1016/j.gloplacha.2019.04.012, 2019.

Zachos, J. C., Quinn, T. M., and Salamy, K. A.: High-resolution (10^4 years) deep-sea foraminiferal stable isotope records of the Eocene-Oligocene climate transition, Paleoceanography, 11, 251–266, https://doi.org/10.1029/96PA00571, 1996.

Zachos, J. C., Dickens, G. R., and Zeebe, R. E.: An early Cenozoic perspective on greenhouse warming and carbon-cycle dynamics, Nature, 451, 279–283, https://doi.org/10.1038/nature06588, 2008.

Zanazzi, A., Kohn, M. J., MacFadden, B. J., and Terry, D. O.: Large temperature drop across the Eocene–Oligocene transition in central North America, Nature, 445, 639–642, https://doi.org/10.1038/nature05551, 2007.